UNIVERSITY OF OKLAHOMA

GRADUATE COLLEGE

CELL WALL ALTERATIONS DURING LATERAL ROOT EMERGENCE IN *ORYZA SATIVA*

A THESIS

SUBMITTED TO THE GRADUATE FACULTY

in partial fulfillment of the requirements for the

Degree of

MASTER OF SCIENCE

By

TIMOTHY JOSEPH PEGG
Norman, Oklahoma
2016

CELL WALL ALTERATIONS DURING LATERAL ROOT EMERGENCE IN *ORYZA SATIVA*

A THESIS APPROVED FOR THE
DEPARTMENT OF MICROBIOLOGY AND PLANT BIOLOGY

BY

_____
Dr. Laura E. Bartley, Chair

_____
Dr. Sharon Kessler

_____
Dr. David McCauley

I’d like to dedicate this research project to my family, friends and mentors who have supported my growth in science and encouraged me to fulfill my potential.

Acknowledgements

I would like to recognize the research opportunity and financial support provided by my graduate advisor Dr. Laura Bartley. I would also like to thank my current and past committee members: Dr. Sharon Kessler, Dr. David McCauley, Dr. Marc Libault, Dr. Richard Mallinson and Dr. Scott Russell for advice and support during my time as a Master's student.

This thesis was dependent on the help and advice from the individuals mentioned below. The University of Oklahoma: Dr. Benjamin E. Smith for training and technical support pertaining to high-resolution confocal microscopy imaging and three-dimensional spatial analysis, Gregory Strout for aid in biological sample preparation and TEM assistance, Dr. Preston Larson for SEM technical and material support, Daniel Jones for fixation protocol recommendations, and Dr. Rosemary Knapp for assistance in cryostat operation and donation of cryopreservation supplies. The Samuel Roberts Noble Foundation: Dr. Jin Nakashima for his microscopy expertise, suggestions regarding RNA collection, and assistance in laser capture microdissection. Complex Carbohydrate Research Center, The University of Georgia: Dr. Michael G. Hahn for the donation of a Monoclonal Antibody Toolkit utilized to label cell wall matrix components with primary antibodies. University of Lyon (France): Dr. Emilie Guillon for the donation of antibodies targeting primary cell walls.

Table of Contents

List of Tables

List of Figures

Introduction

Chapter One

Introduction

An important component of plant root system development is the production of lateral roots originating from older, primary roots (Itoh *et al.*, 2005). Lateral roots are postembryonic structures that form within primary roots and comprise the horizontal component of plant root systems (Tian *et al.*, 2014). Lateral roots are essential for providing plants with water, minerals such as calcium and phosphorous, and anchorage in environments with structurally weak and/or flooded soils (Atkinson *et al.*, 2014). Developing lateral roots, similar to general root system architecture, are able to growth and expand in response to various factors such as nutrient concentrations in the soil, heterogeneity of growth media, and various biotic interactions (Hochholdinger and Zimmermann, 2008). Rice (*Oryza sativa*) is one example of a plant that generates numerous lateral roots from primary root tissue as part of its large, fibrous root system. Specifically, lateral roots typically form in primary seminal and crown root tissue and follow three major developmental steps: pre-initiation, initiation, and post-initiation of lateral root primordia (De Smet *et al.*, 2007).

The pre-initiation step begins in the root cap, the outermost tissue covering root tips which serves as a protective layer for the meristematic cells of the root apex and as a sensory organ that perceives environmental signals such as gravity, water, and nutrients to direct root growth (De Smet, 2012). During root growth, the root cap constantly regenerates new cell layers as superficial layers are shed due to mechanical abrasion experienced by roots as they elongation through growing medium such as soil. When dividing lateral root cap cells extend to the boundaries of the rice root elongation zone (Figure 1) programmed cell death (PCD) occurs and specific groups of root cap cells die

off (Xuan *et al.*, 2016). The PCD of root cap cell groups releases pulses of auxin to surrounding tissues in the root elongation zone. The auxin generated during root cap cell PCD is locally synthesized in the root cap from the conversion of indole-3-butyric acid (IBA) into indole-3-acetic acid (IAA) (De Rybel *et al.*, 2012). Auxin release signals the activation of an oscillating transcriptional mechanism that installs regular spacing of lateral roots in a similar manner to SOMBRERO transcription factor activity observed in Arabidopsis (Fendrych et al., 2014). These regularly spaced cells are referred to as lateral root founder cells (LRFCs) (Vilches-Barro and Maizel, 2015).

After the future location of lateral root primordia is established, the initiation step begins with PIN3-dependent auxin reflux into xylem-pole pericycle cells in LRFC clusters found in developmentally young root tissues, such as maturation zone I in rice. Increased auxin concentration induces the nuclei of at least two xylem-pole pericycles to round up and migrate toward the cell wall common to the two cells (De Rybel *et al.*, 2010). Simultaneously, the pericycle cells swell and overlaying endodermis thins in response to activation of SHY2 auxin repressor proteins in the overlaying endodermis cells (Vermeer *et al.*, 2014). The first anticlinal division of the pericycle cells marks the beginning of both the lateral root primordia, and the auxin gradient that will begin to extend into overlaying cells (Dubrovsky *et al.*, 2001).

Subsequent controlled anticlinal and periclinal cell divisions in the post-initiation stage give rise to the traditional dome-shape of a primordium (Dubrovsky *et al.*, 2000). Further cellular divisions, combined with movement of auxin into overlaying cells by expressed auxin transporters lead to the elongation of the LRP through five different types

of maturation zone root tissues overlaying lateral root primordia: endodermis, cortex (4 layers in rice), sclerenchyma, exodermis, and epidermis.

Establishment of an auxin gradient in the overlaying cells an essential component of the auxin signaling pathway responsible for cell wall enzyme activity in plants such as *Arabidopsis* and rice during lateral root emergence (Figure 3) (Péret *et al.*, 2009). The auxin responsible for signaling in lateral root emergence differs in source from the auxin supply required in the lateral root initiation process. Unlike lateral root initiation, which derives auxin from root cap cells, lateral root emergence utilizes auxin synthesized in shoot tissues (Bhalerao *et al.*, 2002). It is important to note that lateral root primordia will eventually synthesize their own supply of auxin in their root tips, however this auxin source does not play a role in lateral root emergence due to observations of primordial auxin synthesis only occurring after full emergence past primary root tissue layers (Ljung *et al.*, 2005). Auxin derived from shoot tissues typically travels through the phloem and diffuses out into the apoplastic spaces adjacent to plant cell walls (Robert and Friml, 2009). Protonation of auxin in the acidic environment of the cell wall facilitates its movement by diffusion across cell membranes, where it then becomes ionized in the less acidic environment of cellular cytoplasm (Overvoorde *et al.*, 2010). At this point, auxin movement out of the cell becomes limited and requires membrane transport proteins (i.e. auxin transporters) to control directional movement in a processed called “polar auxin transport” (PAT) (Petrášek and Friml, 2009). Ultimately, most auxin will accumulate in the root tip which serves as a major auxin sink tissue. Auxin will then cycle from the meristematic zone of the root tip, through the epidermis to the basal meristem, and then

back towards the root tip via the action of PIN-family auxin efflux transporters located in these cells (Clark *et al.*, 2014).

Utilizing a mechanism observed in *Arabidopsis*, and hypothesized to also exist in cereal grains such as rice (Smith and De Smet, 2012), auxin regulates the lateral root emergence process by mediating the degradation of the transcriptional repressor protein IAA14 through binding of the TIR1 auxin receptor component. TIR1, a type of SCF complex (Skp, Cullin, F-box containing complex), is thought to catalyze the ubiquitination of IAA14 (AUXIN-RESPONSIVE PROTEIN 14) when a sufficient concentration of auxin is present in the cell. Degradation of IAA14 releases its interacting transcription factor, ARF7 (AUXIN RESPONSE FACTOR 7), which then triggers expression of LAX3 (LIKE-AUX3) auxin influx transporters and PIN3 (PIN-FORMED3) auxin efflux transporter (Péret *et al.*, 2013). LAX3 and PIN3 auxin transporter expression is triggered in root cells along the lateral root emergence (LRE) pathway by auxin diffusing from the lateral root primordia initiation site. Auxin transporter expression permits auxin movement, and concentration of auxin, into a distinct gradient in tissues overlaying lateral root primordia to ensure expression of cell wall remodeling proteins such as AUXIN BINDING PROTEIN1 (ABP1) which modulates hemicellulose xyloglucan structure in primary cell walls (Paque *et al.*, 2014). It should be noted, however, that difficulty does exist in the study of lateral root emergence mechanisms due to many genes expressed in both lateral root emergence and lateral root initiation (Vilches-Barro and Maizel, 2015). Specifically, studies which use mutant genes to block or inhibit lateral root initiation, such as *aux1* and *lax3* (Péret *et al.*,

2012), may also inhibit lateral root emergence and cause difficulty in establishing concrete relationships.

In addition to LAX3 and PIN3 auxin transporters, several other genes may play a role in auxin-induced regulation of lateral root emergence. IDA (INFLORESENCE DIFICIENT IN ABSCISSION), HAE (HAESA) and HSL2 (HAESA-LIKE2), previously identified in *Arabidopsis* floral organ abscission (Butenko *et al.*, 2003), appear to induce cell separation of overlaying tissues during lateral root emergence (Kumpf *et al.*, 2013). Specifically, IDA has been identified as a putative signaling peptide that interacts with the leucine-rich repeat, receptor-like kinases HAE and HSL2 present in endodermis cells overlaying developing lateral root primordia. Auxin from developing lateral root primordia induces IDA expression which is followed by signaling through HAE and HSL2 receptors to up-regulate cell wall remodeling genes such as XTR6 (XYLOGLUCAN ENDOTRANSGLYCOSYLASE6), EXP17 (EXPANSIN 17), PGAZAT (PG LATERAL ROOT) and PGLR (PG ABSCISSION ZONE ARABIDOPSIS THALIANA) in cell walls of tissues overlaying lateral root primordia (Kumpf *et al.*, 2013). Auxin influx, via LAX3, into overlaying cells triggers the auxin-dependent cascade leading to the activation of ARF7, which induces expression of IDA, HAE and HSL2 in cells along the lateral root emergence pathway in front of lateral root primordia.

As lateral root primordia development occurs deep within primary roots, remodeling of overlying tissue cell walls is required to accommodate growing primordia during LRE. Previous research involving cell wall remodeling (CWR) induced by the auxin signaling pathway, and IDA-peptide signaling, identified several enzymes

responsible for alterations in plant cell walls (Table 1). For example, xylosyltransferases such as XTR6 (Péret *et al.*, 2013) and XXT1 (Cavalier *et al.*, 2008) both synthesize xyloglucan, which forms a major component of hemicellulose in plant cell walls. Down-regulation of these two genes was observed during lateral root emergence, suggesting that diminished hemicellulose content is required to weaken cell wall structures that may inhibit lateral root primordia elongation. In addition, down-regulation of the genes PRC1, which produces a cellulose synthase required for cellulose microfibril assembly (Fagard *et al.*, 2000), and XEG113, a xyloglucan transferase required to increase cross-linking of extensins in the cell wall matrix (Roycewicz and Malamy, 2014), were similarly observed during lateral root emergence and may also imply that a decrease in specific cell wall component is required for successful LRP emergence.

Other cell wall remodeling enzymes have been identified that destabilize or degrade specific cell wall components. For example, up-regulation of CEL3/GH9B3 (Lewis *et al.*, 2013) and EXP17 (Sato and Miura, 2011) both weaken cell wall structures by either degrading cellulose directly (CEL3/GH9B3), or reducing the cross-linking between cellulose microfibrils to destabilize their position in the cell wall matrix (EXP17). In addition, several enzymes appear to target pectin (e.g. homogalacturonan), another significant structural component of the cell wall, to destabilize the cell wall matrix to permit deformation of cells contacting emerging lateral root primordia. AIR3 (Vilches-Barro and Maizel, 2015), PGLR and PGAZAT (Kumpf *et al.*, 2013) genes yield enzyme products that either act as subtilisin-like serine proteases that degrade homogalacturonan by enabling de-methyl esterification of the pectin backbone and subsequent cleavage by

polygalacturonases (AIR3), or directly serve as polygalacturonases which hydrolyze the bonds between residues in homogalacturonan (PGLR and PGAZAT).

The cell wall itself is a distinguishing feature of plant cells and is critical to the successful development and reproduction of plants. Plant cell walls are commonly divided into two types: primary and secondary. The primary cell wall consists of a rigid layer of complex polysaccharides on the outer surface of the plasma membrane that encases the entire plant cell and changes little after initial synthesis. The secondary cell wall forms underneath the primary cell wall after it has ceased developing and provides additional structural support to plant cells. Unlike primary walls, secondary walls continue to form after the plant cell has ceased expanding and typically exhibit different component ratios than primary cell walls. For instance, secondary cell walls found in xylem and sclerenchyma tissue typically contain significantly more lignin than primary cell walls and serve as strong support structures to ensure proper water transport and maintain overall plant form, respectively.

The primary cell wall is further described according to two distinct classes of cell wall matrix contents: Type-I and Type-II. Dicotyledonous and non-graminaceous monocotyledonous plants possess Type-I cell walls which are characterize as interlinking matrices of xyloglucan and cellulose microfibrils in a hydrated pectin polymer network (Carpita, 1996). Graminaceous monocotyledonous plants, such as rice, possess Type-II cell walls that possess hemicellulose, feruloyated arabinoxylans, and mixed-linkage glucans (1,3; 1,4)-β-D-glucan) as major components with minor quantities of xyloglucans, pectic polysaccharides, and arabinogalactan proteins (Vega-Sánchez *et al.*, 2013)

Remodeling of primary cell wall components is known to occur in overlaying *Zea mays* and *Arabidopsis* root tissues during LRE, but is poorly described in many cereal grains such as *Oryza sativa.* Rice primary wall, similar to other grasses, are characterized by the significant abundance of hemicellulosic polysaccharides, glucuronoarabinoxylans and mixed-linkage glucans, with relatively minor proportions of xyloglucans, pectic polysaccharides, and structural proteins such as arabinogalactan (Pattathil *et al.*, 2015). By contrast, other components such as lignin are located in secondary cell walls that form after primary cell wall development. Modification of these cell wall matrix constituents may influence the properties of the wall matrix such as tensile strength, recalcitrance to enzymatic digestion and proper root elongation (Tenhaken, 2014).

Pectin, a relatively minor primary wall component, is subject to modification in the form of de-methyl esterification of homogalacturonan (Ochoa-Villarreal *et al.*, 2012). Homogalacturonan (HG) itself is the most abundant pectic polysaccharide, constituting ~65% of total pectin in both Type I (dicots) and Type II (commelinoid monocots) plant cell walls. Homogalacturonan consists of a linear α-1,4-linked galacturonic acid (GalA) homopolymer with a typical degree of polymerization of ~100 (Mohnen, 2008). During cell wall synthesis, the homogalacturonan backbone structure is produced in a highly methyl-esterified form from cellular Golgi complex, with methyl-esterification occurring on C2-C3 and C6 GalA residue carbons (Figure 4) (Ridley *et al.*, 2001). Activity from pectinesterases cleave methyl ester bonds later in cell wall development, yielding epitopes of de-methyl esterified pectin homopolymers that play significant roles in overall primary wall integrity (Arancibia and Motsenbocker, 2006).

HG methyl-esterification directly influences structural interactions in plant tissues such as cell wall matrix stability. A “Loosening Model” of primary cell wall alteration suggests that de-methyl esterification enhances the vulnerability of the HG backbone structure to degradation by polygalacturonase enzyme activity – resulting in pectin degradation and a subsequent loss of cell wall matrix structural integrity.

Understanding the developmental changes experienced by cell walls overlaying lateral root primordia can have significant impacts on agricultural research and development, including: expanded knowledge of cereal grain root system development, potential for increases in root system volume, and identification of molecular targets to modify rice cell wall recalcitrance, leading to improvement of rice feedstock digestibility for biofuel production.

To better understand developmental changes during rice LRE, immunohistochemical studies were performed on sectioned root tissue from rice root seedlings. Antibody binding patterns from these results identified epitopes of primary cell wall components that appear to be modified in cells near the primordium during LRE. Further testing with enzymatic assays illuminated the potential chemical interactions between select cell wall components during lateral root emergence. In addition, groundwork for future relative gene expression and transcriptome analysis of tissues subject to cell wall matrix alterations was initiated with the development of an optimized laser capture microdissection protocol for rice root tissue.

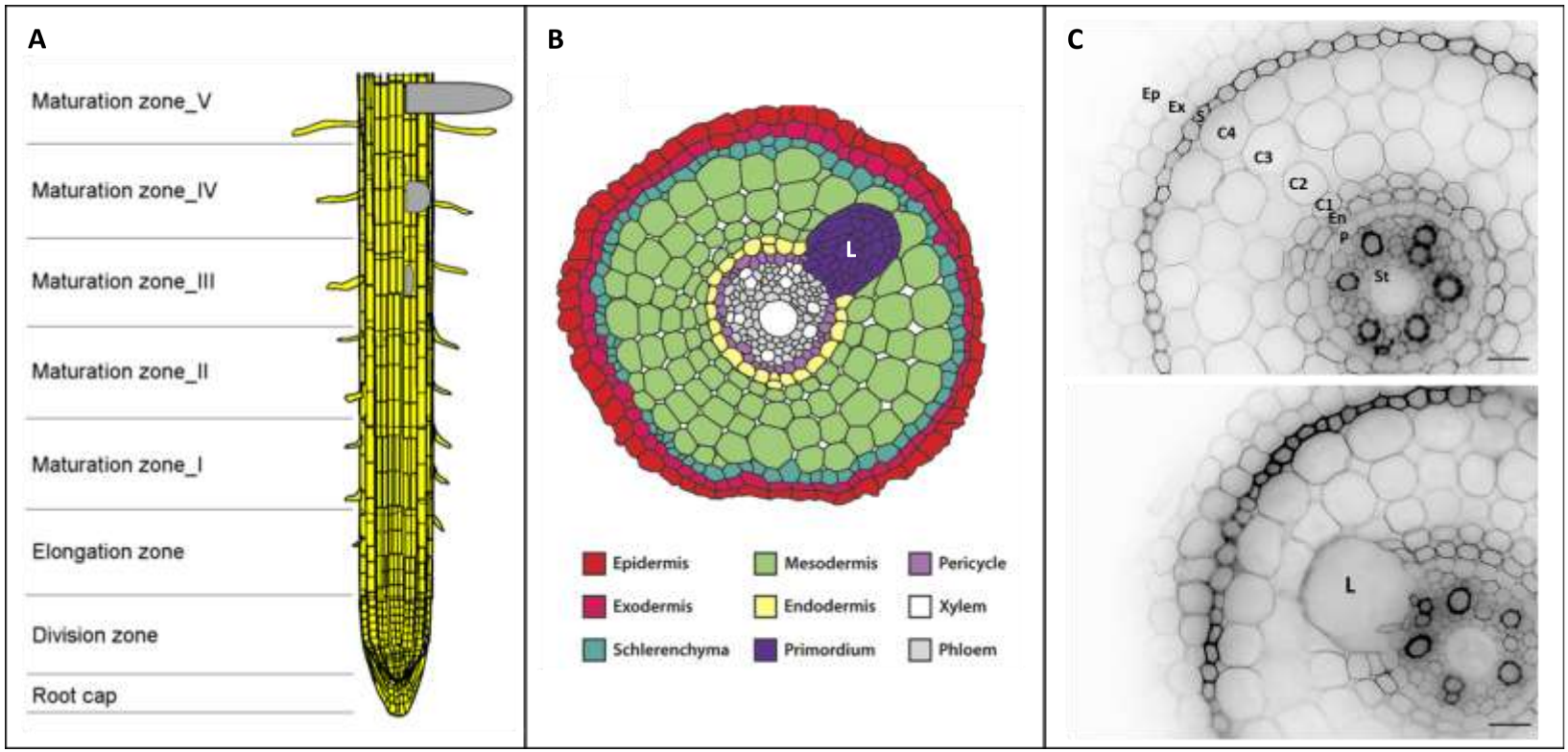
A
Maturation zone_V
Maturation zone_IV
Maturation zone_III
Maturation zone_II
Maturation zone_I
Elongation zone
Division zone
Root cap
B
L
Epidermis
Exodermis
Schlerenchyma
Mesodermis
Endodermis
Primordium
Pericycle
Xylem
Phloem
C
Ep
Ex
S
C4
C3
C2
C1
En
P
St
L

Figure 1 - Rice crown root developmental regions and tissues.

(A) Schematic representation of rice crown roots consisting of eight developmental regions (Sato *et al.*, 2010). (B) Schematic representation of a rice root cross sections with lateral root primordium (L) and six distinct tissue layers (Péret *et al.*, 2013). (C) Cross sections of rice root tissue layers with lateral root primordium (top) and without primordium (bottom). Images are micrographs of false-colored signals (inverted-gray LUT value) of native cell wall autofluorescence. Ep – epidermis; Ex – exodermis; S – sclerenchyma; C4 – 4th cortical layer; C3 – 3rd cortical layer; C2 – 2nd cortical layer; C1 – 1st cortical layer; En – endodermis; P – pericycle; St – stele (vascular tissues). Bars = 20 µm

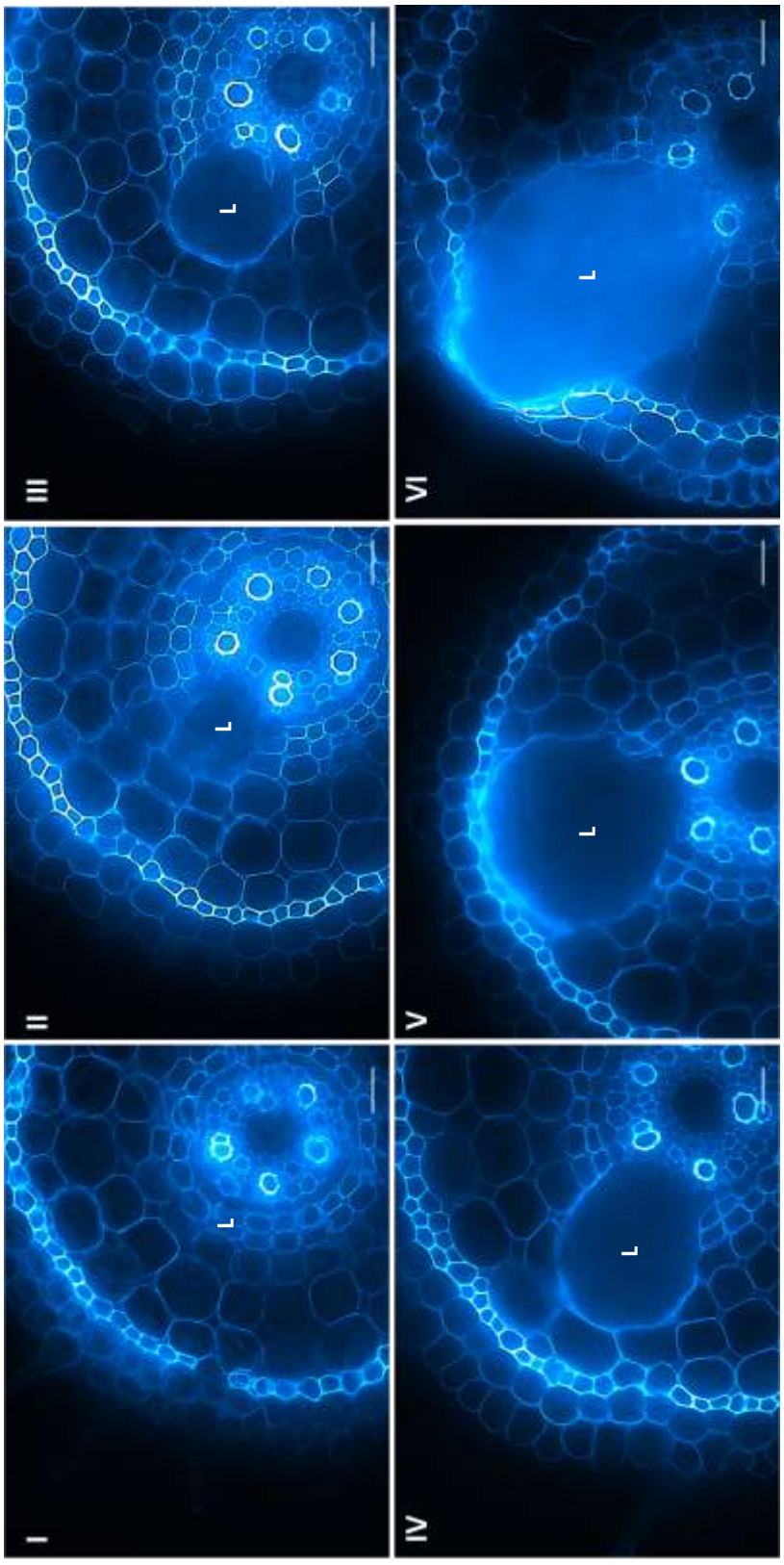
I
II
III
IV
V
VI

Figure 2 - Developmental stages of lateral root emergence in rice

(I) Rice lateral root emergence (LRE) begins with lateral root primordia (L) initiating in the crown root pericycle layer and elongating towards the endodermis, which is identified as Stage I due to limitations in identifying earlier stages. (II-IV) Stage II-IV LRE is denoted by the primordia apex encountering the each of the four cortical cell layers found in maturation zone developmental tissue. (V) Stage V LRE in a brief stage observed during primordia contact with the sclerenchyma layer. (VI) Stage VI LRE is observed during primordia contact with the exodermis. LRE later than Stage 6 is not recorded due to occasional absence or damage to epidermal layer in tissue sections. Images are micrographs of false-colored signals from native cell wall autofluorescence (cyan). Bars = 20 μm.

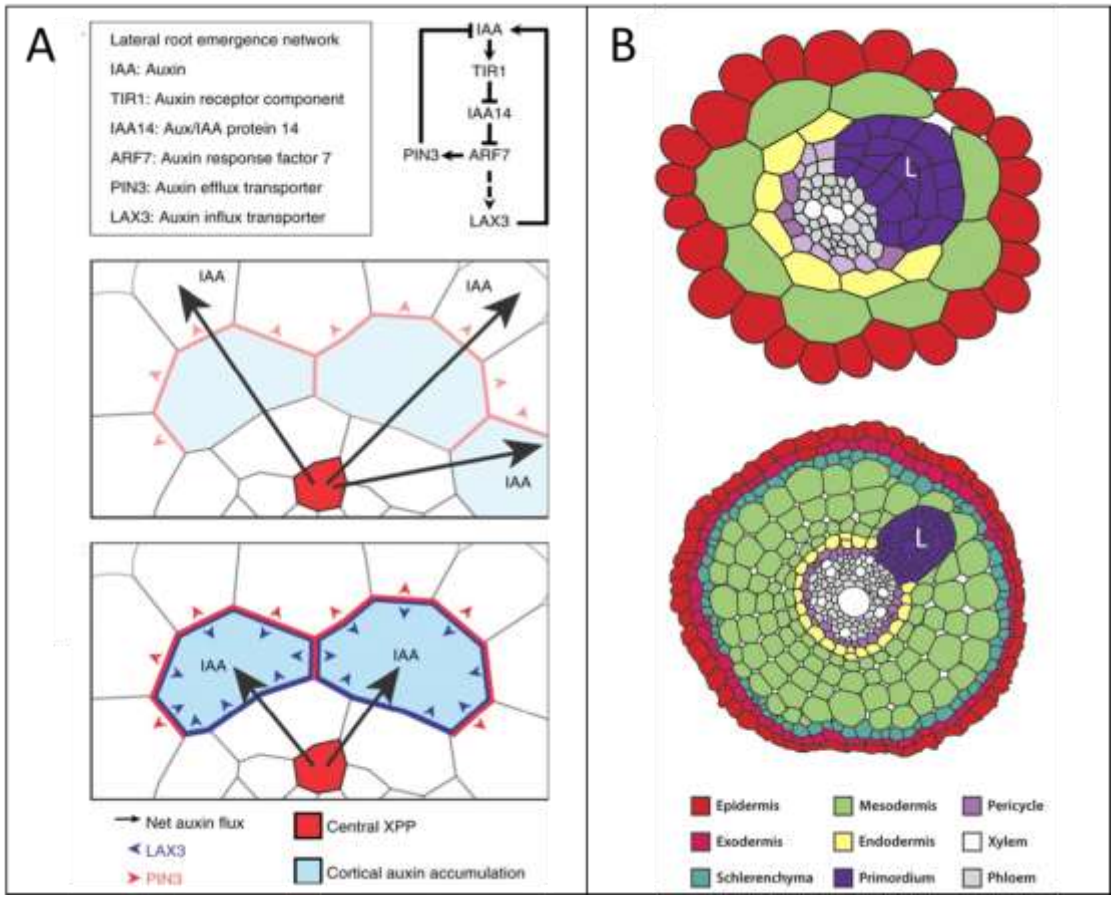

Figure 1 - Hypothesized regulation of lateral root emergence in root tissues

(A) Lateral root formation and elongation relies on an elaborate auxin signaling pathway regulated by an auxin response factors, signaling protein and auxin transporters which function to create an auxin gradient in cells immediately overlaying developing lateral root primordia. (B) Comparison of *Arabidopsis thaliana* and rice tissue layers suggests the hypothesized LRE model in *Arabidopsis* will be similar to the uncharacterized LRE model of rice. (Reproduced with permission from (Péret *et al.*, 2013) and (Swarup *et al.*, 2008)).

Table 1: Select Genes of Interest Involving in Cell Wall Remodeling during Lateral Root Emergence

Gene	Product	Function	Reference
AIR3 (AUXIN-INDUCED IN ROOT CULTURES3)	Subtilisin-like serine protease	Processes pectin methylesterase enzymes into an active form. Enables de-methyl esterification of pectin in cell wall and increasing polygalacturonase enzyme susceptibility.	(Vilches-Barro and Maizel, 2015)
XTR6 (Xyloglucan α-xylosyltransferases 6)	Xylosyltransferase	Synthesizes xyloglucan. Maintains cell wall stability via cellulose-hemicellulose crosslinking.	(Péret *et al.*, 2013)
CEL3/GH9B3 *(*CELLULASE3/GLYCOSYLHYDROLASE9B3*)*	Glycoside hydrolase 9 family enzyme	Catalyzes cellulose microfibril breakdown, leading to cell wall loosening.	(Lewis *et al.*, 2013)
XEG113 (Xyloglucotransferase113)	Xyloglucan transferase	Induces arabinosylation of cell wall extensins. Increases extension cross-linking and cell wall strength.	(Roycewicz and Malamy, 2014)
PRC1 (PROCUSTE1)	Cellulose Synthase	Creates cellulose microfibrils required for to form cell wall matrix. Required for root cell elongation.	(Fagard *et al.*, 2000)
XXT1 (Xyloglucan α-xylosyltransferases 1)	Xylosyltransferase	Synthesizes xyloglucan. Maintains cell wall stability via cellulose-hemicellulose crosslinking.	(Cavalier *et al.*, 2008)
EXP17 (Expansin 17)	Expansin	Causes relaxation in cell wall mechanical stress by loosening linkages between cellulose microfibrils.	(Sato and Miura, 2011)
PGLR (PG LATERAL ROOT)	Polygalacturonase	Cleaves homogalacturonan backbone of pectin. Destabilization of primary cell wall and middle lamella.	(Kumpf *et al.*, 2013)
PGAZAT (PG ABSCISSION ZONE ARABIDOPSIS THALIANA)	Polygalacturonase	Cleaves homogalacturonan backbone of pectin. Destabilization of primary cell wall and middle lamella.	(Kumpf *et al.*, 2013)

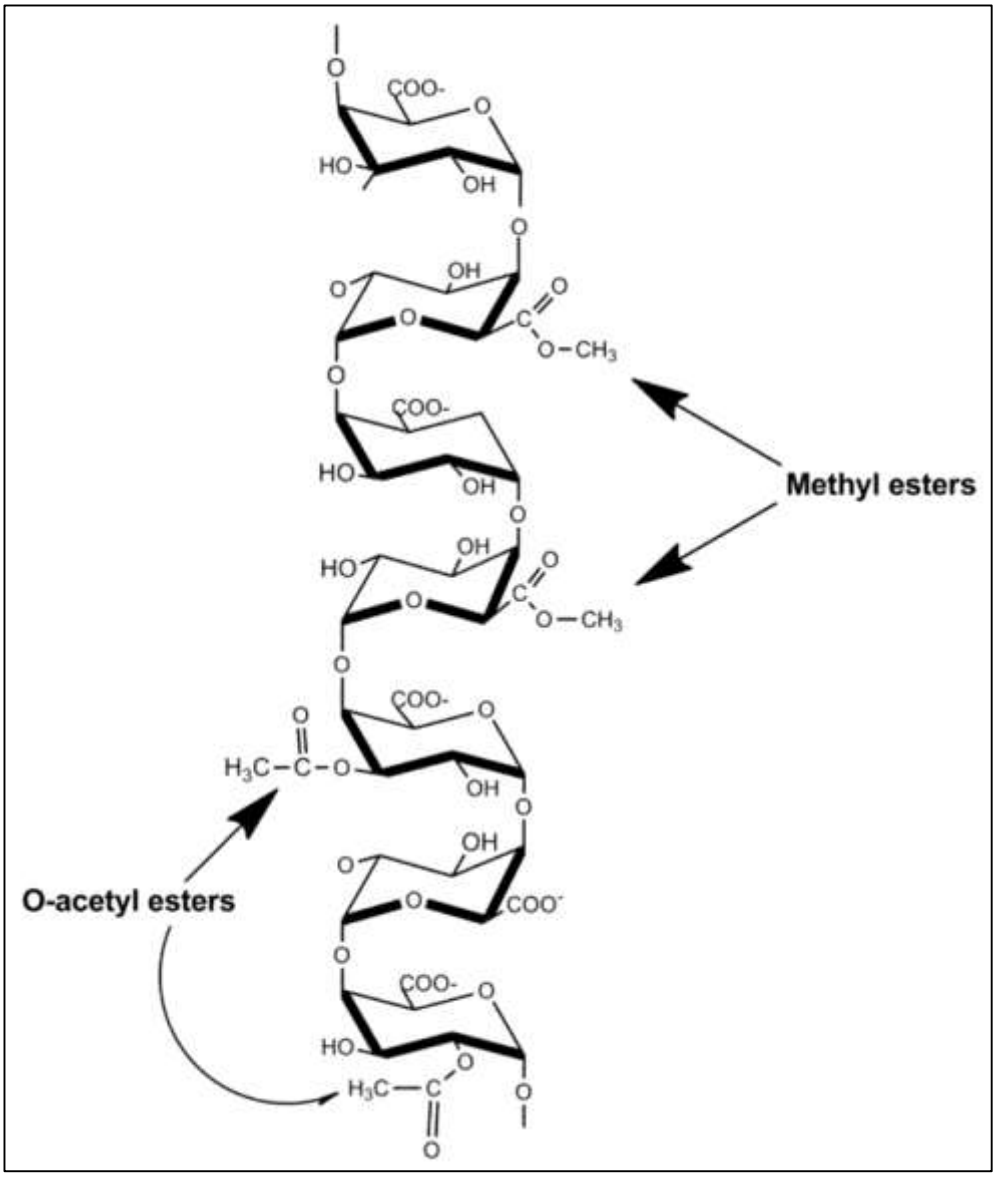

Figure 2 - Structure of homogalacturonan

As the backbone structure of most pectic polysaccharides, homogalacturonan consists of linear polymers comprised of 1→4 linked α-d-Gal***p***A residues. Some of the carboxylates of the Gal***p***A residues are esterified with methanol. The Gal***p***A residues may also be esterified with acetic acid at C2 and C3. Image usage under Creative Commons License 3.0. (Ochoa-Villarreal *et al.*, 2012).

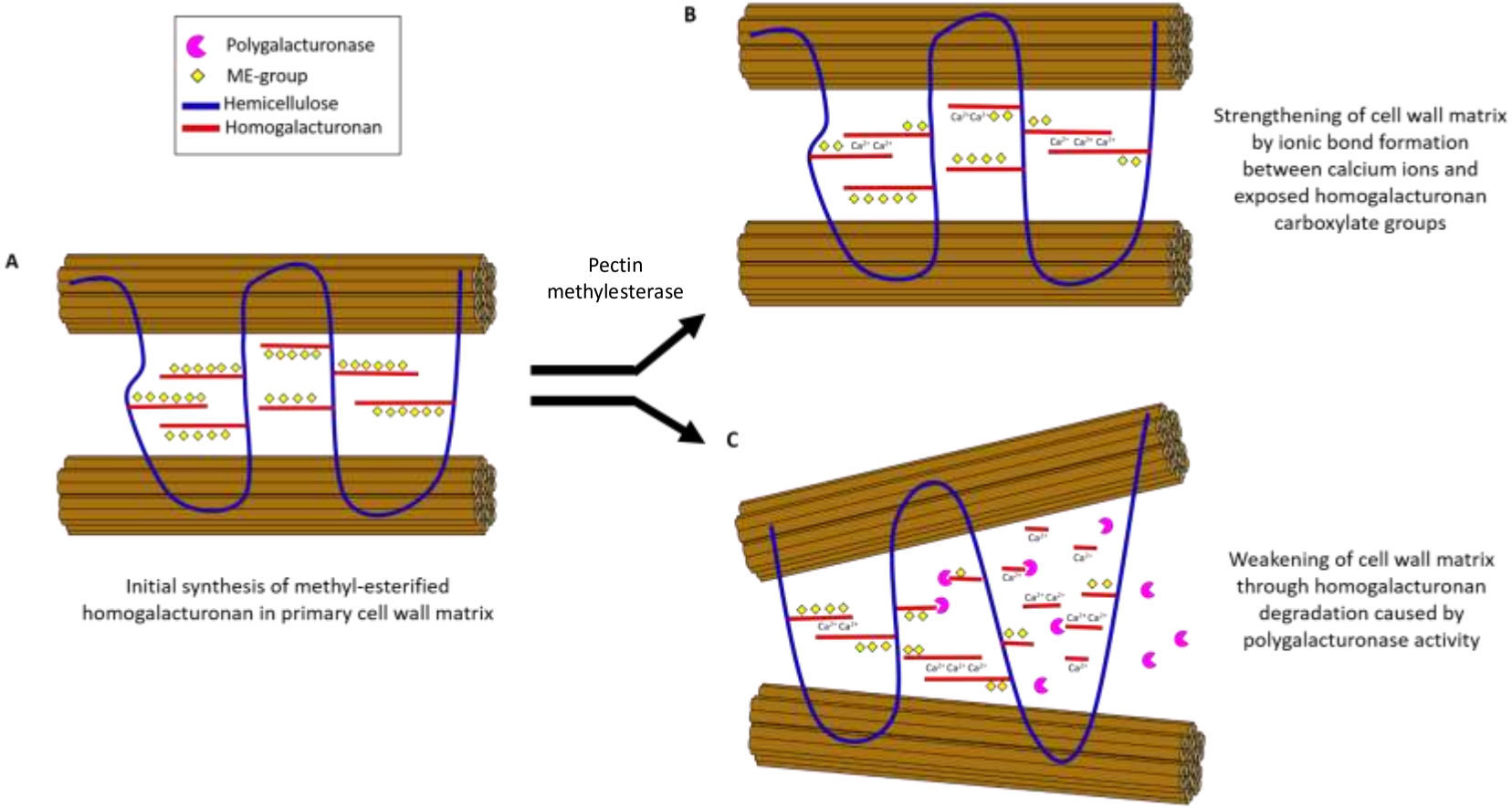
Polygalacturonase
ME-group
Hemicellulose
Homogalacturonan
A
Initial synthesis of methyl-esterified homogalacturonan in primary cell wall matrix
Pectin methylesterase
B
Strengthening of cell wall matrix by ionic bond formation between calcium ions and exposed homogalacturonan carboxylate groups
C
Weakening of cell wall matrix through homogalacturonan degradation caused by polygalacturonase activity

Figure 3 - "Loosening Model" of primary cell wall destabilization

(A) Homogalacturonan is synthesized in the cellular Golgi and transported to the primary cell walls in a highly methyl-esterified form with multiple methyl groups (yellow) substituted to the D-galacturonic acid backbone (red) which is covalently linked to hemicellulose polymers (blue). (B) After de-methyl esterification occurs calcium ions (Ca^{2+}) bind to adjacent homogalacturonan strands with exposed carboxylate ions, forming an "egg-box" cross-linking structure that strengthens the cell wall matrix. (C) Degradation of the homogalacturonan backbone occurs due to polygalacturonase activity permitted by cross-linking structures. Loss of homogalacturonan creates instability in hemicellulose structures, and changes alignment of cellulose microfibrils (brown) in the primary cell wall matrix. Overall structure of the cell wall matrix weakens and become increasingly malleable to mechanical stress.

Chapter 1: Microscopic evaluation of primary cell wall polysaccharide alterations during lateral root emergence in *Oryza sativa*

1-1 Background

Cell walls are important support structures synthesized during mitotic division of plant cells and are typically characterized as tough, rigid matrix formations comprised of various cell wall polymers and proteins. Plant cells may possess two types of cell walls: primary and secondary. The primary cell wall does not significantly alter composition or physical dimensions after initial synthesis, except in specific types of plant development such as seed shattering (Christiansen *et al.*, 2002), leaf abscission (Agustí *et al.*, 2009), floral organ abscission (Aalen *et al.*, 2013), and fruit ripening (Goulao and Oliveira, 2008). These developmental events typically entail an alteration of select cell wall components in order to weaken overall primary cell wall structure. Secondary cell walls, by contrast, are formed after maturation of primary cell walls and may continue synthesizing cell wall matrix components, such as lignin and cellulose, to provide additional mechanical strength to plant cell walls (Cosgrove and Jarvis, 2012). Many dynamic changes to primary cell wall structure are often found to be due to alterations in pectic polysaccharide composition and localization within the cell wall matrix (Abasolo *et al.*, 2009).

Pectins are structurally complex, highly soluble components in the cell wall, making up ≤10% of the primary wall of grasses and other commelinoid plants (Scheller *et al.*, 2007). Pectins are a covalently linked galacturonic acid (GalA) rich cell wall polysaccharide family (Albersheim et al., 1996; Mohnen, 2008) consisting of three

different types of polysaccharide domains: homogalacturonan (HG), rhamnogalacturonan I (RG-I) and rhamnogalacturonan II (RG-II). Homogalacturonan forms the backbone of most pectic polysaccharides as a linear chain of 1,4 linked α-D- galacturonic acid residues that comprises ~65% of pectin (Mohnen, 2008). Rhamnogalacturonan I is a branched polymer consisting of a backbone of a repeating disaccharide of [- 4)-α-D-galacturonic acid- (1,2)-α-L-rhamnose-(1-] with side chains predominantly comprising arabinofuranosyl and galactopyranosyl residues and representing 20-35% of total cell wall pectin (Ridley *et al.*, 2001). Rhamnogalacturonan-II, the most structurally complex pectin, consists of a backbone of linear 1,4-linked α-D-GalA residues, with four different side chains consisting of 12 unique glycosyl residues linked to more than 20 different linkages and representing only about 10-15% of the pectin (O'Neill *et al.*, 2004).

The homogalacturonan backbone is known to be altered during cell wall remodeling and may serve as an measure of developmental events in plant tissues (Wolf *et al.*, 2009).The primary mechanism of pectin alteration appears to be caused by the de-methyl esterification of the homogalacturonan backbone structure and subsequent changes in covalent bonding interactions between other cell wall matrix components. Initially, de-methyl esterification of homogalacturonan exposes carboxylate groups on the pectin backbone structure to ionic bonding with calcium ions (Ca^{2+}) already present in the cell wall (Kader and Lindberg, 2010). Four oxygen atoms from exposed carboxyl groups on two adjacent HG polymer will then form ionic bonds with a single calcium ion to create a polymer cross-linking structure referred to as the “egg-box model” (Plazinski, 2011). The structure egg-box model results in the tight packing of HG polymers and the ability to bind at least four molecules of water for calcium ion bound, resulting in

subsequent pectin gelling often observed in plant primary cell walls (Braccini and Pérez, 2001). The egg-box model is also suspected to permit crosslinking to hemicellulose components, such as xyloglucan, leading to the pectin gel matrix complementing the role cellulose-xyloglucan complexes in maintaining primary wall integrity (Caffall and Mohnen, 2009).

On the other hand, the presence of de-methyl esterified homogalacturonan within the egg-box structures induces pectin-hydrolyzing enzyme activity in the form of polygalacturonase and pectin/pectate lyases (Wolf *et al.*, 2009). Increased polygalacturonase activity within cell walls is theorized to disrupt pectin matrix structure and induce alterations in plant cell dimensions, similar to changes in stigma and style structure during pollen tube development in plants such as *Larix decidua* (Rafińska *et al.*, 2014). The contradictory nature of a strong pectin egg-box structure leading to subsequent pectin hydrolysis activity supports assumptions of the dynamic primary cell wall components that are remodeled depending on developmental requirement within plant tissues and/or exposure to outside, abiotic factors (Willats *et al.*, 2006). In addition, changes in calcium-mediated HG crosslinking often contribute to changes in cell wall properties during plant development (Willats *et al.*, 2001). The parallel or antiparallel arrangement of cross-linked HG polymers is known to be a significant source of cell wall tensile strength (Caffall and Mohnen, 2009).

In the current study, a combination of immunolabeling, enzymatic treatment and structured illumination microscopy of rice root tissue cross sections provided significant compositional information regarding the various tissue layers overlaying rice lateral root primordia that develop after preliminary lateral root initiation. Alterations in cell wall

matrix components, such as hemicellulose and pectin, were examined in order to shed light on the possible interactions of different primary wall polymers. Data from the current study was used to evaluate previously reported models of primary cell wall remodeling and apply them to explain cellular accommodation of growing LRP in developmentally mature rice root tissues.

1-2 Methods

Plant growth conditions and developmental staging

Developing seedlings of rice (*Oryza sativa* cv. *Dongjin*) were grown under fluorescent lighting in a 25^{o}C incubator. Rice were harvested from sealed petri dishes six days after initial seed germination in ½ strength Murashige and Skoog (MS) media, pH 6.5. Seedlings were harvested based on the presence of 2-3 crown roots, and no emerged lateral roots in maturation zone tissues.

Root tissue harvesting and sectioning

Crown root sections were cut from six-day old seedlings in deionized water under a standard dissection microscope. Unfixed crown root sections from maturation zones I & II were cut into 1 cm sections prior to embedding in 3.5% agarose blocks (Henry *et al.*, 2016). Approximately 5-6 root segments were embedded in each agarose block prior to sectioning on Vibratome-1000 (Ted Pella, Inc.) at 50 µm thickness.

Immunolabeling of root cross sections

Agarose-embedded root sections were chosen based on the presence of lateral root primordia. 3-6 rice root sections were placed in a 1.5 mL Eppendorf tube. Samples were washed for ten minutes, three times, in 10 mM Tris-Buffer Saline solution with 0.1% Tween-20 (TBST). Approximately 250 µL of cell-wall specific monoclonal antibody, diluted either 1/10 or 1/20 strength in 1X TBST buffer, was placed in each sample tube and followed with a 12 hour incubation period at 4 ^{o}C. After the incubation period, samples washed again with 10 mM TBST buffer. Diluted goat secondary antibody

(1/500) conjugated to Alexa Fluor™ 647 fluorophore was added to the samples based upon the requirements of the primary antibodies (Table 2). Sections were washed a final 3 times in 10 mM TBST, prior mounting in miowol mounting media between two Golden Seal® No. 0 coverslips. Autofluorescence of the root tissue was imaged with a 40X dry objective on a Zeiss ApoTome structured illuminated microscope under an 488 nm excitation wavelength, while 633 nm excitation was used for secondary antibodies conjugated to Alexa Fluor ® 647.

Enzymatic Treatments

Rice root sections (50 µm) were incubated for two hours at 25^{o}C using reagents from the Novozyme Cellulosic Ethanol Enzyme Kit. Enzyme concentrations were created using the following maximum suggested % w/w according to the manufacturer recommendations: Cellulase complex (NS22086) = 5%, Xylanase (NS22083) = 0.25%, β-glucosidase (NS22118) = 0.6%, and Enzyme complex (NS22119) = 0.4%. Pectin lyase (AN2569) and pectin methyl esterase (AN3390) enzymes, donated by the Mort Lab of Oklahoma State University, were diluted 1/10 in deionized water to concentrations of 0.062 U/mL and 0.011 U/mL, respectively. Lichenase (10 U/mL) was also separately incubated with samples for 2 hours at room temperature.

Image Rendering

Image rendering was performed using ImageJ (NIH, Bethesda). Fluorescence images for native autofluorescence and fluorophore-conjugated secondary antibody were processed with either a Gaussian Blur plugin (low pass filter) to increase standard deviation of pixel

distribution and smooth image appearance, or an UnsharpMask plugin (high pass filter) to rescale blurry images and sharpen visual quality. Fluorescence images for their respective channels (secondary antibody fluorophore, or native autofluorescence) were combined into z-series stacks and normalized to the standard mean intensity of each stack using the Bleach Correction plugin (EMBL Heidelberg). The following lookup table (LUT) values were chosen to improve visual clarity of antibody binding patterns of immunolabeling and enzyme treatment images: magenta (Alexa Fluor® 647 fluorophore) and green (cell wall native autofluorescence).

1-3 Results

Autofluorescence of rice crown root tissue sections during lateral root emergence

Rice root tissue cross sections demonstrate autofluorescence in the green-blue wavelengths of the visible light spectrum upon exposure to ultraviolet excitation. Autofluorescence is noticeable in all tissue layers including root stele (xylem and phloem), pericycle, endodermis, cortical cells (four layers), sclerenchyma, exodermis, and epidermis. Fluorescence microscopy revealed changes in native autofluorescence intensity of sclerenchyma tissue layers overlaying lateral root primordia (LRP) during three developmental stages of lateral root emergence (LRE) (Figure 1.1). Reduced fluorescence was directly observed in 4-5 contiguous sclerenchyma cells walls apical to the lateral root primordium emergence pathway. Changes in fluorescence signal may suggest a decrease or alteration of phenolic compounds including ferulic acid, *p*-coumaric acid and/or lignin, all of which fluoresce when exposed to ultraviolet light (Harris and Hartley, 1976).

Immunofluorescent labelling of crown root tissue sections

Initial antibody screening investigated the presence of select cell wall components in rice root tissues by evaluating changes in fluorescence signal in cells near lateral root primordia. Evaluation of fluorescence signal due to antibody binding was classified under one of three types: no signal, no change in signal compared to rice root tissue areas not overlaying a lateral root primordium, and localized increase in signal near lateral root primordium.

Antibody labeling of select cell wall component epitopes demonstrated no changes in fluorescent signals in tissues overlaying emerging lateral root primordia (Figure 1.2). Antibodies for de-methyl esterified homogalacturonan with greater than four degrees of polymerization (CCRC-M38) (Figure 1.3), methyl-esterified homogalacturonan at least five residues long (CCRC-M130) (Figure 1.4), rhamnogalacturonan I backbone structure (CCRC-M14) (Figure 1.5), and arabinoxylan (LM11) indicated strong localization in cortical tissue layer cells throughout the entire rice root cross section with the exception of LM11, which displayed strong antibody binding in lateral root primordia and all xylem tissue of the rice root stele (Figure 1.6). These results were confirmed in root section replicates demonstrating Stage III-IV lateral root emergence.

Unique antibody binding patterns were observed for six antibodies targeting major cell wall components (Figure 1.7). Treatment with INRA-COU1 (Tranquet *et al.*, 2009) for free para-coumaric acid and para-coumarate esters (Figure 1.8) and CCRC-M100 for xyloglucan epitope, XXXG, (Figure 1.9) revealed increased fluorescent antibody binding signals in exodermis, sclerenchyma and cortical tissue cells overlaying lateral root primordia. Increased signal was observed at between 1-4 cell files in advance of the lateral root primordia apex during Stage III-V lateral root emergence for each antibody.

LM19 for de-methyl esterified homogalacturonan (Figure 1.10), JIM5 (Figure 1.11) and CCRC-M34 for partially de-methyl esterified homogalacturonan (Figure 1.12), and LM20 for methyl-esterified homogalacturonan (Figure 1.13) revealed no change in antibody binding signal in all cortical tissues observed during Stage I-VI lateral root

emergence. However, 20-50 µm wide sclerenchyma and exodermis cells sections overlaying lateral root primordia displayed increased signal intensity compared to other sections of the rice root tissue during Stage I-VI LRE. The presence of antibody binding signals was detected up to 6 cell files away from the lateral root primordia apex at Stage I, implying that some form of signaling mechanism is revealing or synthesizing epitopes for specific cell wall components far in advance of the lateral root primordia.

LM19 localization pattern alteration during enzymatic treatments

Evaluation of the antibody binding pattern for de-methyl esterified homogalacturonan (LM19) was conducted utilizing a series of eight enzyme treatments: enzyme complex mixture, cellulase complex mixture, xylanase, pectin lyase, pectinesterase, sodium carbonate (pH 11.4), β-glucosidase (Figure 1.14). The objective of these treatments was to determine the influence of selective cell wall component removal on the availability of the LM19 epitope, and suggest possible dependencies between de-methyl esterified pectin and major cell wall components such as cellulose and hemicellulose.

Positive control treatment with sodium carbonate (pH 11.4) displayed no significant alterations to the LM19 binding pattern. Sodium carbonate treatment served as a positive control in the enzyme assay experiments due to reported enhancement of de-methyl esterified homogalacturonan availability via cleavage of methyl-ester bonds and excision of methyl groups from the backbone structure (Hervé *et al.*, 2011). The resulting binding pattern observed from the sodium carbonate treatment verified the proper activity

of the LM19 antibody, and served as a useful comparison when evaluating potential binding pattern changes between different enzyme treatments.

Negative control treatments using enzyme complex enzymes and pectin lyase treatments both yielded predictable results with a loss of LM19 binding pattern in sclerenchyma and exodermis due to degradation of all major cell wall components by assorted enzyme complex enzymes, or targeted hydrolysis of the homogalacturonan backbone structure (pectin lyase), which removes epitope structures needed for LM19 binding (Jia *et al.*, 2009). An absence of signal intensity in all cells overlaying lateral root primordia as well as diminished fluorescence signal in the primordia. Due to the natural autofluorescence of lateral root primordia overlapping the emission wavelength of the Alexa Fluor® 647 secondary antibody fluorophore, changes in lateral root primordia signal intensity may imply alteration of the LM19 binding epitope and/or degradation of naturally autofluorescent cell wall components.

Treatment with cellulase complex mixture and xylanase, resulted in the severe reduction, and possible elimination, of antibody binding signals in sclerenchyma and exodermis cells at least two tissue layers in front of lateral root primordia during Stage V lateral root emergence. Treatment with cellulase enzymes in the cellulase complex mixture was used to determine if the cleavage of 1,4-β-D-glucosidic linkages in the cellulose microfibrils of the cell wall would render the antibody binding epitope unrecognizable, possibly through the shifting of cell wall matric component alignments which is hypothesized to occur when such an important cell wall polymer is removed. The endoxylanase enzyme contained within the xylanase treatment was used to evaluate the effect of hydrolytic degradation of hemicellulose, via cleavage of linear β-1,4-xylan

polysaccharides into D-xylose (Zverlov *et al.*, 2005), on the ability of LM19 to bind to its pectin epitope and provide support to a possible relationship between hemicellulose and pectin during lateral root emergence.

Treatment of rice tissue sections with β-glucosidase and lichenase served as a method to investigate the potential relationship between LM19 binding and cleavage of cellobiose, a disaccharide of glucose that is found in cellulose (Teugjas and Väljamäe, 2013), and mixed linkage glucans, a major component of rice cell walls (Xue and Fry, 2012), respectively. The standard LM19 fluorescent signal was observed for both enzyme treatments in overlaying exodermis and sclerenchyma tissues 1-2 cell layers in advance of developing LRP, and in cortical, endodermis and stele phloem tissues throughout the rice root cross-section.

1-4 Discussion

Localization of primary cell wall epitopes revealed by immunofluorescent labelling

The current study sought to evaluate three possible models of cell wall deformation during lateral root emergence in order to explain changes experienced by cells overlaying lateral root primordia. To this end, we created three models of rice lateral root emergence to propose the following changes to cell wall components: (i) general degradation of all major cell wall components in tissues overlaying LRP, (ii) synthesis of new cell wall components that alter the compositional ratio of the cell wall matrix and (iii) remodeling and modification of select cell wall components during LRE.

In the current study, fluorescence microscopy revealed changes in native autofluorescence of rice root tissues which may support Model I. Reduction of fluorescence signal intensity of sclerenchyma tissue layers overlaying lateral root primordia (LRP) during three lateral root emergence (LRE) developmental stages (Figure 1.1) suggests the possibility of general cell wall degradation. Previous literature partially supports this hypothesis due to the known fluorescence of phenolic cell wall compounds such as ferulic acid, *p*-coumaric acid and/or lignin when exposed to ultraviolet light (Harris and Hartley, 1976). Degradation of lignin in rice root tissues is also implied in the antibody binding signal for free para-coumaric acid and para-coumarate esters (INRA-COU1). Incubation with INRA-COU1 antibody revealed increase fluorescence signals in cortical, sclerenchyma and exodermis cells overlaying lateral root primordia in multiple stages of development (Figure 1.2), potentially suggests the degradation of lignin. However, the presence of unbound *p*-coumaric acid or *p*-coumarate esters in front of developing lateral root primordia may also imply other possibilities: partial degradation

of lignin cross-linking enabling primary antibody binding to released *p*-coumaric acid, alteration to lignin structure enable binding of *p*-coumaric acids/esters, or removal of another cell wall component(s) that unmasks the antibody binding site.

Another possibility suggested by the INRA-COU1 binding pattern is synthesis of free *p*-coumaric acid or *p*-coumarate esters in overlaying cell walls during lateral root emergence. Support for cell wall component synthesis postulated by Model II is observed in overlapping fluorescent signals for antibody labeling of INRA-COU1 and CCRC-M100 (xyloglucan). Both antibody labeling treatments only demonstrated signal localization in cortical, sclerenchyma and exodermis root cell layers in front of emerging lateral roots. These results imply that synthesis of *p*-coumaric acid, *p*-coumarate esters and xyloglucan may be essential in enabling successful deformation of cell walls destined to contact lateral root primordia.

The binding pattern of xyloglucan is particular interesting since xyloglucan is known to form an important part of cellulose-hemicellulose structures in primary cell walls. Xyloglucan typically consists of β-1,4-linked glucopyranosyl residues substituted with xylosyl groups at regular intervals (dos Santos *et al.*, 2015). This structure enables xyloglucan to tightly associate with cellulose in both Type I and Type II plant cell walls (Carpita and Gibeaut, 1993). During cellulose biosynthesis the xyloglucan backbone structure becomes entrapped by cellulose microfibril in primary cell walls (Pauly *et al.*, 1999). The distribution of the antibody binding pattern may suggest synthesis of large amounts of xyloglucan (supporting Model II) which would prevent complete entrapment by cellulose microfibrils and destabilize the structure of the cellulose-hemicellulose cross-linking structure. As a result, xyloglucan epitopes would be available for CCRC-

M100 binding and cell wall matrix structure would be weakened to permit cell wall deformation during lateral root emergence.

However, another possibility entails degradation of xyloglucan itself, which would weaken the covalent and non-covalent bonds hemicellulose shares with the pectic polysaccharides (Abasolo *et al.*, 2009) and lead to possible destabilization of the pectin matrix in primary cell walls. This type of selective degradation or modification of cell wall components may provide significant support for Model III.

Previous literature suggests covalent interactions exist between xyloglucan and pectin (Caffall and Mohnen, 2009) in addition to known cellulose/xyloglucan binding structures in plant primary walls. An immunofluorescent screening of select pectin epitopes (Table 2) was performed to evaluate hypothesized xyloglucan-pectin relationships. Specifically, antibodies for two epitopes de-methyl esterified homogalacturonan (LM19, CCRC-M38), two epitopes of partially methyl-esterified homogalacturonan (JIM5 and CCRC-M34) and two epitopes of methyl-esterified homogalacturonan (LM20, CCRC-M130) were tested to determine if binding pattern overlaps with xyloglucan (CCRC-M100) could be observed. Consistent binding of sclerenchyma and exodermis layers in LRP-containing root cross sections were observed in multiple LRE developmental stages for LM19, JIM5, CCRC-M34, and LM20, which overlapped with previously seen patterns in CCRC-M100 and INRA-COU1. However, we observed that CCRC-M38 and CCRC-M130 epitopes of homogalacturonan may not be present in front of emerging LRP, suggesting that modification of homogalacturonan yields very specific residues during LRE (Table 2).

In addition, differing degrees of de-methyl esterification or methyl-esterification in homogalacturonan-targeting antibodies appear to have no impact in number or location of antibody labeled cells (Figure 1.15). These results imply that epitopes for LM19, JIM5, CCRC-M34 and LM20 exist simultaneously in cells during most stages of lateral root emergence, supporting the premise of a dynamic cell wall experiencing constant chemical remodeling activities. In addition, since the limitations of the immunofluorescent cannot conclusively determine is the pectin binding pattern is cause by synthesis of more pectin epitopes, or removal of another cell wall component "masking" the LM19, JIM5, CCRC-M34 and LM20 epitopes, the experimental data may support both Model II and Model III alterations to cell wall composition.

The high degree of fluorescent signal overlap observed between antibodies implies that remodeling of major cell wall components, such as cellulose, may disrupt cell wall matrix cross-linking and shift epitope recognition sites for pectins, xyloglucan and free *p*-coumaric acid and/or *p*-coumarate esters enough to enable successful primary antibody binding. Similarity of binding patterns supports the hypothesis of active cell wall remodeling, due to antibody localization mimicking expected auxin distribution patterns preceding developing LRP (Péret *et al.*, 2012). A possible concentration gradient of auxin signaling molecules in cells preceding developing LRP is likely responsible for triggering cell wall remodeling enzyme synthesis at early stages of LRE (Péret *et al.*, 2012). This hypothesis is supported by known interactions between hemicellulose, cellulose, lignin and pectin, along with noticeable reduction in sclerenchyma tissue native autofluorescence that was observed in sample from every antibody treatment.

Influence of cell wall component degradation on LM19 localization pattern

The enzymatic assay treatment displayed several alterations to the tissue localization pattern for normally seen in LM19 antibody binding, and implied several relationships that supported Model III for lateral root emergence. Specifically, the selective removal of cell wall components by certain enzyme treatments appeared to disrupt the ability of the LM19 monoclonal antibody to bind to the de-methyl esterified homogalacturonan epitope structure in sclerenchyma and exodermis tissue layers (Figure 1.14).

Removal of the LM19 binding pattern was also observed by treatment with the cellulase complex enzyme mixture. Treatment with cellulase enzymes in the cellulase complex mixture suggests that the cleavage of cellulose 1,4-β-D-glucosidic linkages renders the antibody binding epitope unrecognizable, and/or removes de-methyl esterified homogalacturonan in cell walls near lateral root primordia (LRP). This result is surprising since previous research reported that the cellulose-xyloglucan network of the primary wall is structurally independent from the pectin matrix, with removal of one network leaving the other components unaffected (Carpita and Gibeaut, 1993). However, it is known that removal of pectins in primary walls can influence the mobility of cellulose and xyloglucan without resulting component loss from the cell wall matrix (Iain *et al.*, 1990). This possibility is also suggested based on antibody binding results for CCRC-M100 which implies liberation of xyloglucan from cross-linking interactions with cellulose, without necessarily altering xyloglucan chemical structure.

In addition, xylanase treatment demonstrated a significant reduction of LM19 binding in rice root exodermis and sclerenchyma tissue. The influence of hemicellulose

degradation on antibody binding of de-methyl esterified homogalacturonan is expected due to known covalent binding between pectins and hemicellulose components of the primary cell wall (Cosgrove, 2005).

Further treatment with β-glucosidase, and lichenase enzymes implied little relationship between the de-methyl esterified homogalacturonan epitope of LM19 and cellobiose or mixed-linkage glucan (MLG) components of rice root cell walls. Lack of influence of cellobiose degradation on de-methyl esterified homogalacturonan epitope availability may be due to the requirement of endoglucanase and exoglucanase activity to degrade cellulose into cellobiose residues for β-glucosidase to act upon. Another possibility is that direct binding between cellulose and pectins does not occur, and instead relies on another component (i.e. hemicellulose) to bind them into a functional cell wall matrix. The interaction of MLGs with cellulose, hemicellulose and pectin in primary cell walls is unknown, despite reported correlation of high MLGs content with active cell growth and cellular expansion (Vogel, 2008). As a result, no influence on the LM19 de-methyl esterified homogalacturonan epitope may occur, despite a possible increase of MLGs themselves in cells undergoing other remodeling during LRE.

Overall enzyme binding results, along with antibody labeling data, supports both Model II (synthesis of cell wall components in cells overlaying LRP) and Model III (selective component degradation) activities during lateral root emergence. Furthermore, these hypothetical models, in addition to experimental results, support a "Loosening Model" of lateral root emergence which suggests cellulose-hemicellulose-pectin interactions provide a stable cell wall matrix that is gradually disrupted via de-methyl esterification of homogalacturonan, and subsequent polygalacturonase activity, prior to

contact with emerging lateral root primordia (Figure 1.16). Removal of cellulose and hemicellulose (xylan) from the cell wall apparently leads to the degradation of de-methyl esterified homogalacturonan epitopes, or prevents homogalacturonan modification from even occurring by degrading the backbone structures itself.

Experimental data also provides support for the "Loss of Cellular Adhesion Model" of primary cell wall destabilization during lateral root emergence (Figure 1.17). Specifically, enzymatic degradation of homogalacturonan with pectin lyase and pectinesterase, combined with data demonstrating localized primary antibody labeling of sclerenchyma and exodermis tissues in specific homogalacturonan epitopes, suggests that de-methyl esterification of pectin is necessary to destabilize the pectin matrix in middle lamella and permit separation of adjacent cells in order to accommodate LRP emerging through rice root tissues. Similar mechanisms have been described in plants that experience softening and separation of cell walls, such as ripening fruit (Wakabayashi *et al.*, 2003). In addition, support for polygalacturonase activity in the "Loss of Cellular Adhesion Model" has been described in a recent report on cellular separation during abscission of floral organs in *Arabidopsis* (Aalen *et al.*, 2013).

Future research questions will relate to why overlapping fluorescent antibody binding patterns were seen in tissue overlaying lateral root primordia, but no significant loss of fluorescent signal was detected in any previous immunofluorescent assay. A possible explanation is that only specific epitopes of cell wall components such as cellulose or hemicellulose may be removed in cells apical to emerging lateral root primordia. Testing new primary antibodies to cell wall components, such as LM10 for xylan (Chen *et al.*), may reveal diminished or absent binding patterns in cells near lateral

root primordia. Reduction in fluorescent signal may suggest alteration of hemicellulose epitopes during the enzymatic digestion of pectin predicted in the "Cell Wall Loosening" model and provide support for the hypothesized hemicellulose destabilization in the primary cell wall matrix.

Another question to be answered is how to evaluate possible synthesis of cell wall components in rice root cell walls during LRE. Possible experimentation may involve immunolabeling of rice root sections from loss of function mutants for pectin galacturonosyltransferase (GAUTs) with antibodies for de-methyl esterified homogalacturonan (e.g. LM19) and methyl-esterified homogalacturonan (e.g. LM20). An absence or severe reduction of antibody binding in cells apical to lateral root primordia in sclerenchyma and exodermis tissue layers would support the hypothesis that synthesis of cell wall components, such as homogalacturonan, may be responsible for some antibody binding patterns observed in rice root tissues. These results would suggest that cell wall component synthesis, in addition to component modification, may occur in cells overlaying LRP during lateral root emergence.

1-5 Conclusion

Modifications of cell wall matrix components may suggest a need for dynamic primary wall composition in order for cells in rice roots to accommodate newly formed organs. Analysis of cellular changes during lateral root emergence stages indicates relatively low abundance compounds such as homogalacturonan, xyloglucan and *p*-coumaric acid are significantly altered in sclerenchyma and exodermis cells destined to physically contact elongating lateral root primordia. Enzymatic removal of select cell wall polysaccharides suggests potential structural interaction between cellulose, hemicellulose and de-methyl esterified pectic polysaccharides within the primary cell wall. Further research is still required to evaluate potential interactions between other epitopes of methyl-esterified or de-methyl esterified homogalacturonan, and rice primary cell wall components such as lignin, mixed-linkage glucans, and hydroxycinnamic acids.

Determining the genetic mechanism of primary wall modification and remodeling during rice lateral root emergence may shed light on the regulation of cell wall matrix mechanical properties. For example, confirming the presence of IDA-mediated peptide signaling in rice root tissues could reveal a cell wall remodeling mechanism common to both lateral root emergence and floral abscission processes (Kumpf *et al.*, 2013). A possible future experiment could then be designed to test the effects of constitutively overexpressing components of the IDA-HAE/HSL2 signaling module, throughout rice plant tissue (i.e. shoots, roots, etc.). Possible results may include significantly reduced cell wall recalcitrance, which would be of economic significance due to the status of rice as a potential biofuel feedstock (van der Weijde *et al.*, 2013).

In addition, future research involving selective modification and/or decrease of cell wall components such as lignin, cellulose, pectins and hemicellulose may yield additional avenues for creating transgenic rice with reduced cell wall recalcitrance. Specifically, autofluorescence data implied the possibility of lignin reduction in sclerenchyma tissue cell walls overlaying emerging lateral root primordia. Due to the increased malleability of cell walls in the lateral root emergence pathway, interruption of the lignin biosynthesis pathway by inhibition of enzymes such as CINNAMATE 4-HYDROXYLASE (C4H), *p*-COUMARATE 3-HYDROXYLASE (C3H), and FERULATE 5-HYDROXYLASE (F5H) (Vanholme *et al.*, 2010) may destabilize secondary cell wall structure and explain how lateral root primordia are able to distort strong structural tissues, such as sclerenchyma, in the root tissue. Light microscopy methods developed in this study may be used to confirm decrease in lignin by evaluating rice root sections for any loss of autofluorescent signal.

Table 2. Monoclonal Primary Antibody List

Antibody Name	Isotype	Host	Immunogen	Antigen	Epitope Structure
LM11	IgM	Rat	Xylopentaose-BSA conjugate	Xylan, Arabinoxylan	beta-Xyl-(1->4)-beta-Xyl-(1->4)-beta-Xyl-(1->4)-beta-Xyl
LM19	IgM	Rat	Fruit pectic galacturonan	Homogalacturonan	-alpha-GalA(1-4)alpha-GalA(1-4)alpha-GalA(1-4)alpha-GalA
LM20	IgM	Rat	Seed Mucilage	Homogalacturonan	alpha-MeGalA(1-4)alpha-MeGalA(1-4)alpha-MeGalA(1-4)alpha-MeGalA
CCRC-M14	IgM	Mouse	Rhamnogalacturonan I backbone	Rhamnogalacturonan I backbone	-2-alpha-Rha1-4-alpha-GalA1-2-alpha-Rha1-4-alpha-GalA1-2-alpha-Rha1-
CCRC-M34	IgM	Mouse	Homogalacturonan (partially methyl-esterified)	Homogalacturonan (partially methyl-esterified)	Base-sensitive homogalacturonan epitope
CCRC-M38	IgG1	Mouse	Seed mucilage/MeBSA complex (Non-covalent)	Homogalacturonan	De-esterified HG (DP > 4) epitope
CCRC-M100	IgM	Mouse	Xyloglucan/BSA (covalent)	Xyloglucan	XXXG
CCRC-M130	IgG1	Mouse	Pectin/MeBSA (non-covalent)	Homogalacturonan	Me-Homogalacturonan epitope
JIM5	IgG2a	Rat	Protoplast prepared from suspension-cultured cells	Homogalacturonan (partially methyl-esterified)	Me(alpha)GalA1→4(alpha)GalA1→4(alpha)GalA1→4(alpha)GalA1→4(alpha)GalA1→4(alpha)MeGalA

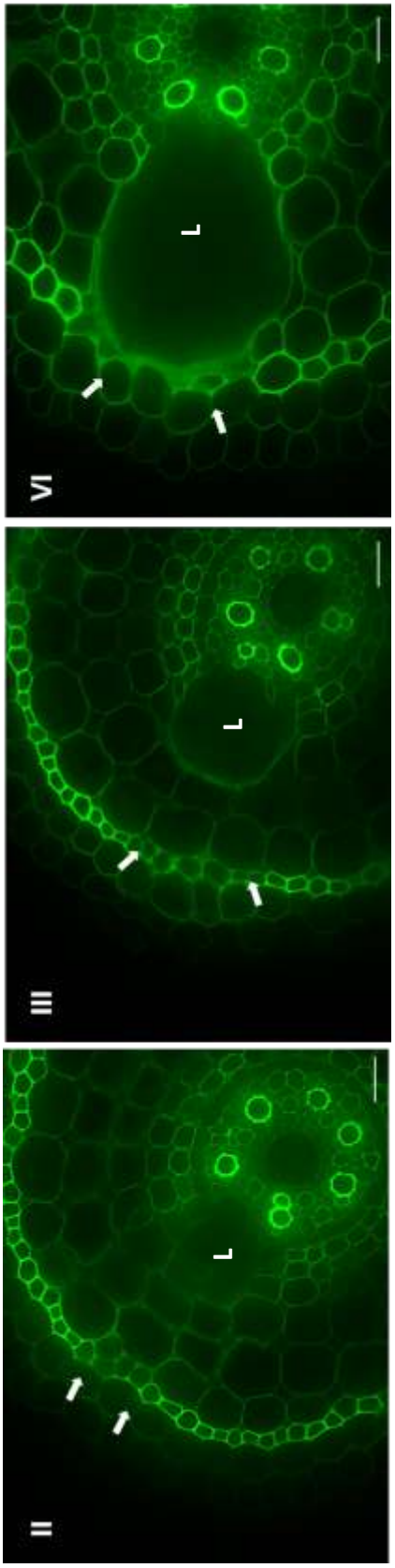
VI
III
II

Figure 1.1 – Decrease of native autofluorescence during lateral root emergence in rice (II-IV) Native cell wall autofluorescence diminishes in sclerenchyma tissue (white arrows) in front of emerging lateral roots (L). Images are false-colored with red/green LUT table values to emphasize fluorescence intensity. Stage II, Stage III and Stage IV lateral root images are shown from unique crown root section. Bars = 20 µm.

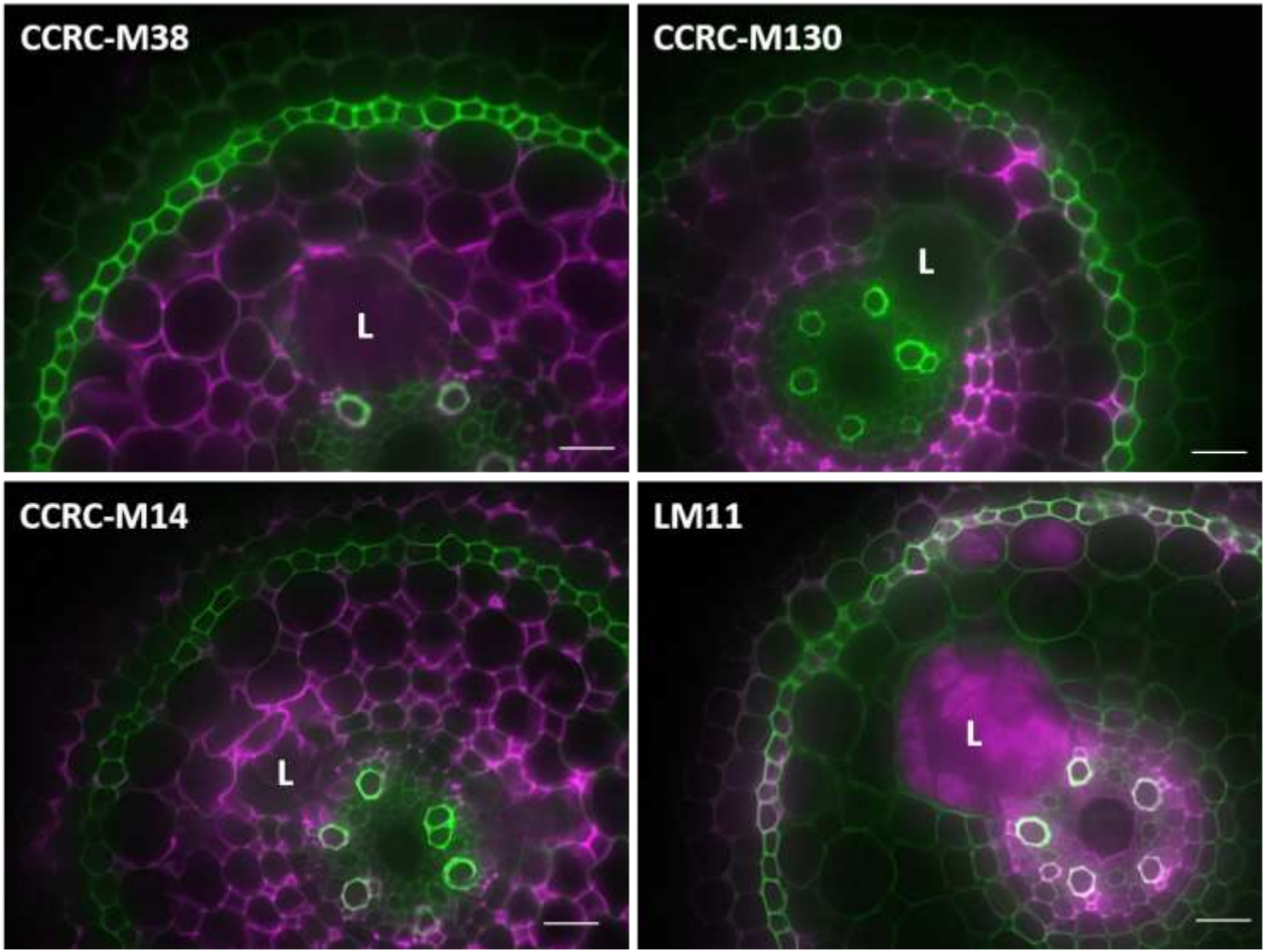
CCRC-M38
L
CCRC-M130
L
CCRC-M14
L
LM11
L

Figure 1.2 – No change of primary antibody binding in tissues overlaying lateral root primordia. Sclerenchyma and exodermis tissue overlaying the emerging lateral root primordium (L) demonstrate no Alexa Fluor® 647 fluorescence binding pattern and suggest an absence of de-esterified homogalacturonan (CCRC-M38), methyl-esterified homogalacturonan (CCRC-M130), rhamnogalacturonan I (CCRC-M14), and arabinoxylan (LM11) in Stage III-IV rice lateral root emergence. Images are composite micrographs of false-colored signals from autofluorescence (green) and AlexaFluor647-conjugated secondary antibody (magenta). Bar = 20 μm.

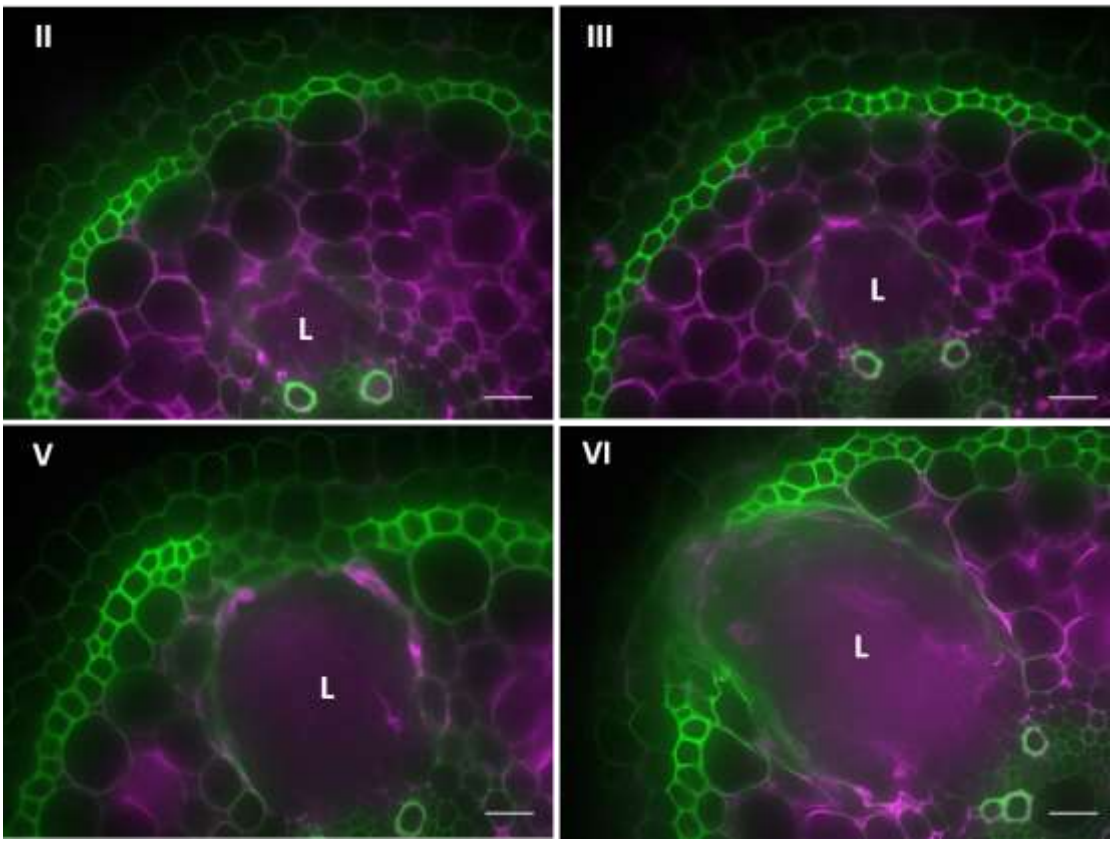

Figure 1.3 - Labeling of de-methyl esterified homogalacturonan with CCRC-38 monoclonal antibody (II-VI) Cortical cells and emerging lateral root primordium (L) demonstrate the presence of de-methyl esterified homogalacturonan (degree of polymerization >5) across four lateral root emergence stages in rice. Images are composite micrographs of false-colored signals from autofluorescence (green) and AlexaFluor647-conjugated secondary antibody (magenta). Bar = 20 µm.

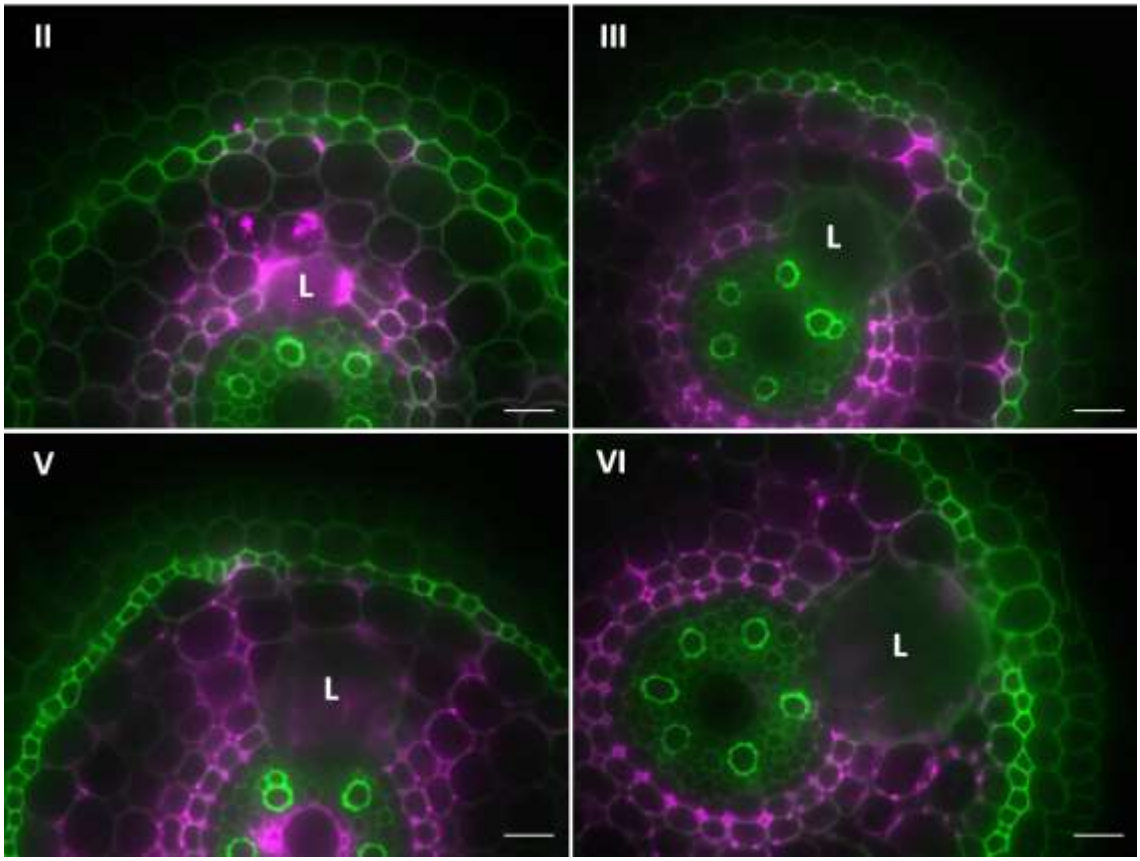

Figure 1.4 - Labeling of methyl-esterified homogalacturonan with CCRC-130 monoclonal antibody (II-V) Cortical tissue adjacent to the emerging lateral root primordium (L) demonstrates the presence of methyl-esterified homogalacturonan across four lateral root emergence stages in rice. No binding pattern is observed in front of the lateral root primordia in sclerenchyma and exodermis layers. Images are composite micrographs of false-colored signals from autofluorescence (green) and AlexaFluor647-conjugated secondary antibody (magenta). Bar = 20 µm.

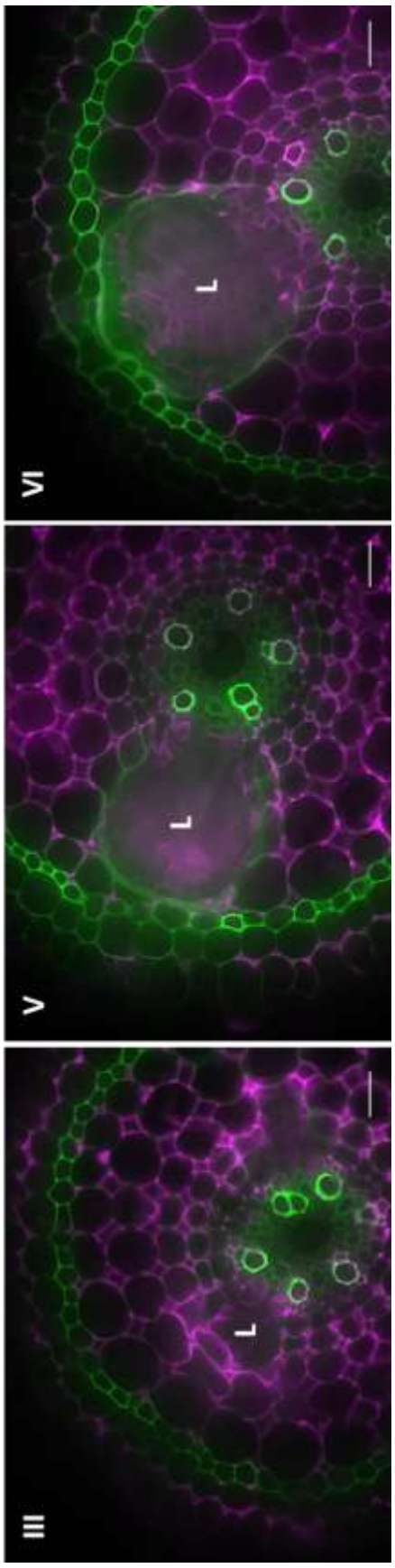
VI
L
V
L
III
L

Figure 1.5 - Labeling of rhamnogalacturonan I with CCRC-M14 monoclonal antibody (III, V, VI) Cortical tissue, endodermis and pericycle layers demonstrate the presence of the rhamnogalacturonan I backbone structure across three lateral root emergence stages in rice. Sclerenchyma and exodermis tissue overlying the emerging lateral root primordium (L) display no secondary antibody (Alexa Fluor® 647 fluorophore) fluorescence pattern. Images are composite micrographs of false-colored signals from native autofluorescence (green) and AlexaFluor647-conjugated secondary antibody (magenta). Bar = 20 μm.

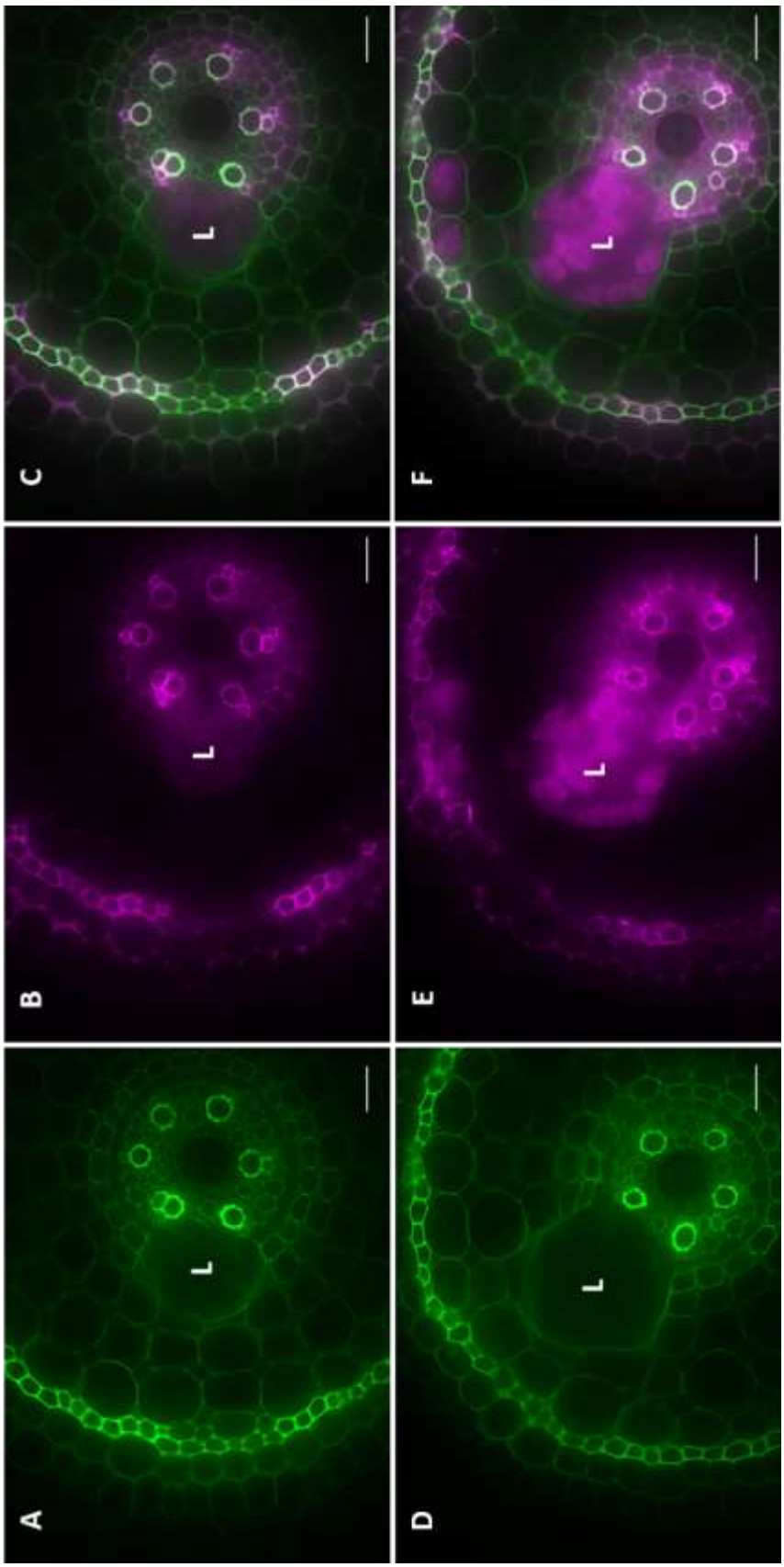
A
L
B
L
C
L
D
L
E
L
F
L

Figure 1.6 - Binding pattern of rice root arabinoxylan with LM11 monoclonal antibody (A-C) Sclerenchyma and exodermis tissues overlying the emerging lateral root primordium (L) demonstrate an absence of arabinoxylan during Stage II lateral root emergence in rice. (D-F) LM11 binding pattern is still visible during Stage IV lateral root emergence stages. Images are micrographs of false-colored signals from autofluorescence (green) and AlexaFluor647-conjugated secondary antibody (magenta). Composite images (C, F) were created from overlaying green and magenta channels. Bar = 20 μm.

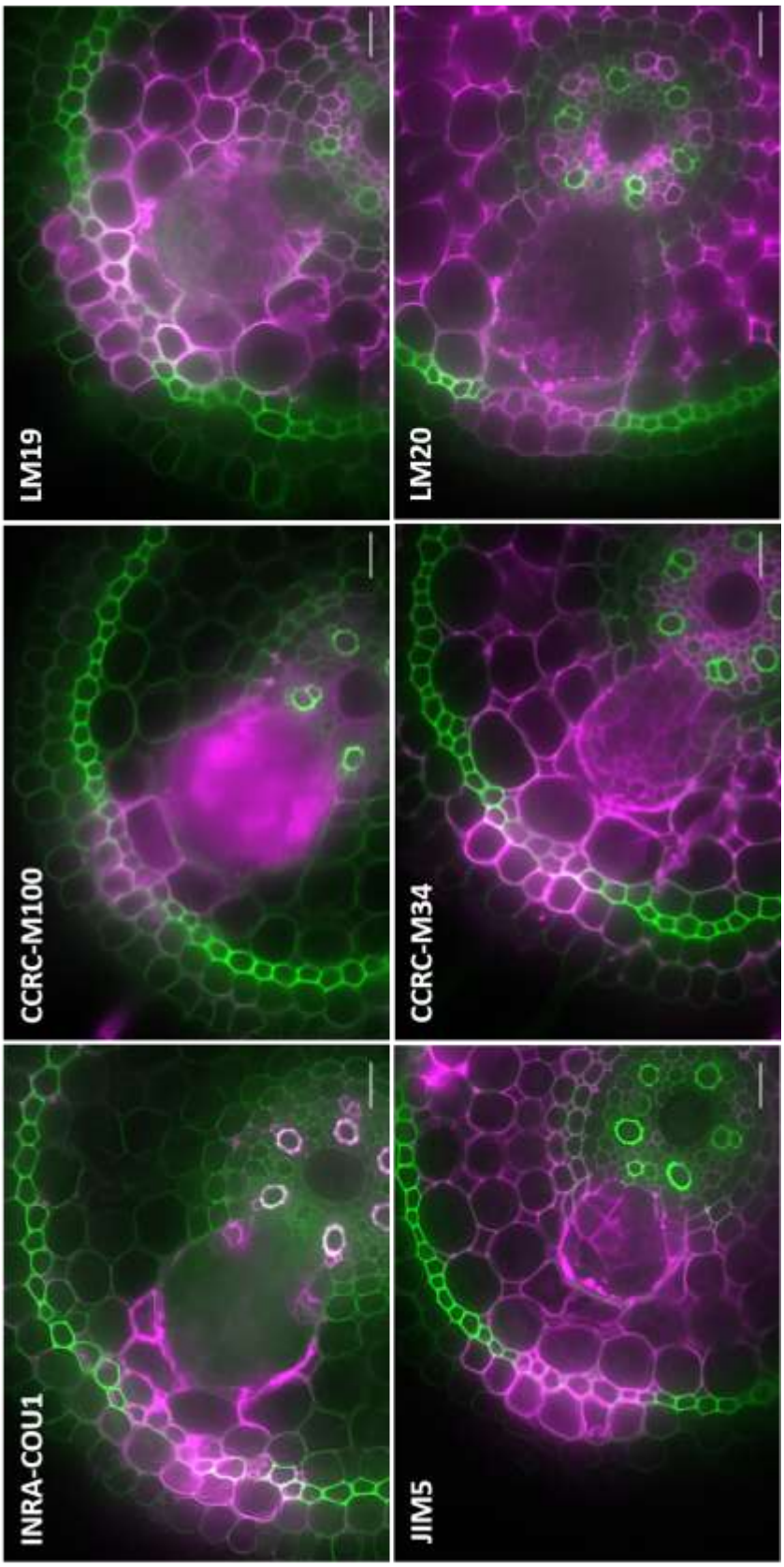
LM19
CCRC-M100
INRA-COU1
LM20
CCRC-M34
JIM5

Figure 1.7 – Localization of select cell wall components in tissues overlaying the lateral root primordium. Schlerenchyma and exodermis tissue overlaying the emerging lateral root primordium (L) demonstrates the presence of free para-coumaric acid (INRA-COU1), a xyloglucan epitope (CCRC-M100), de-methyl esterified homogalacturonan (LM19), partially methyl-esterified homogalacturonan (JIM5 & CCRC-M34), and methyl-esterified homogalacturonan (LM20) near Stage IV lateral root emergence stages in rice. Images are composite micrographs of false-colored signals from autofluorescence (green) and AlexaFluor647-conjugated secondary antibody (magenta). Bar = 20 µm.

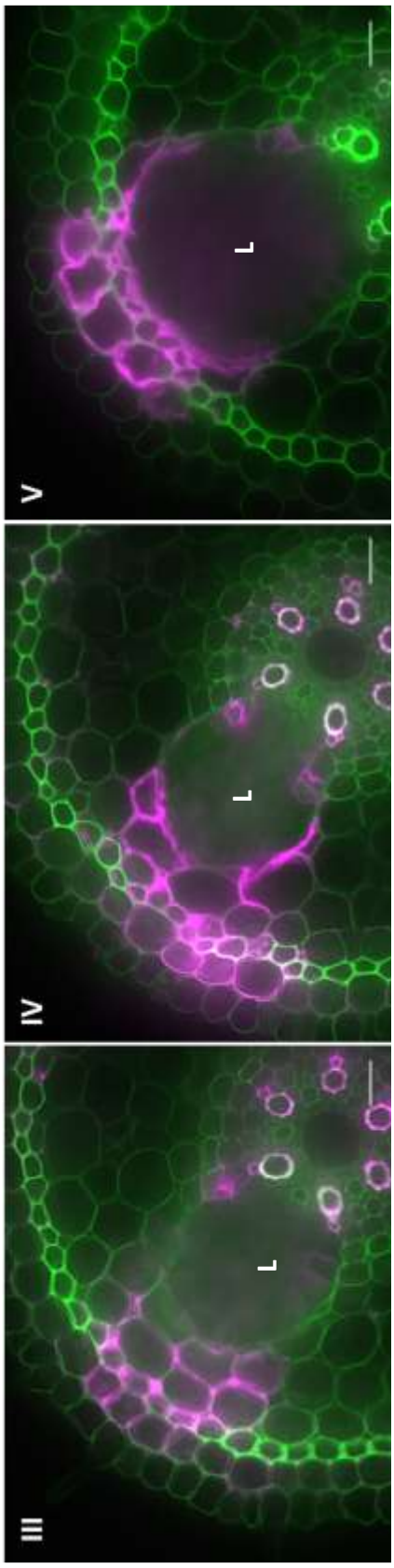
V
IV
III

Figure 1.8 - Labeling of free para-coumaric acid with INRA-COU1 (III-V) Sclerenchyma and exodermis tissue overlaying the emerging lateral root primordium (L) demonstrates the presence of free para-coumaric acid and/or para-coumarate esters across three lateral root emergence stages in rice. Observed developmental stages show contact of the lateral root primordium apex with cortical layer 3 (Stage III), cortical layer 4 (Stage IV), and sclerenchyma layer (Stage V) tissues. Images are composite micrographs of false-colored signals from autofluorescence (green) and AlexaFluor647-conjugated secondary antibody (magenta). Bar = 20 µm.

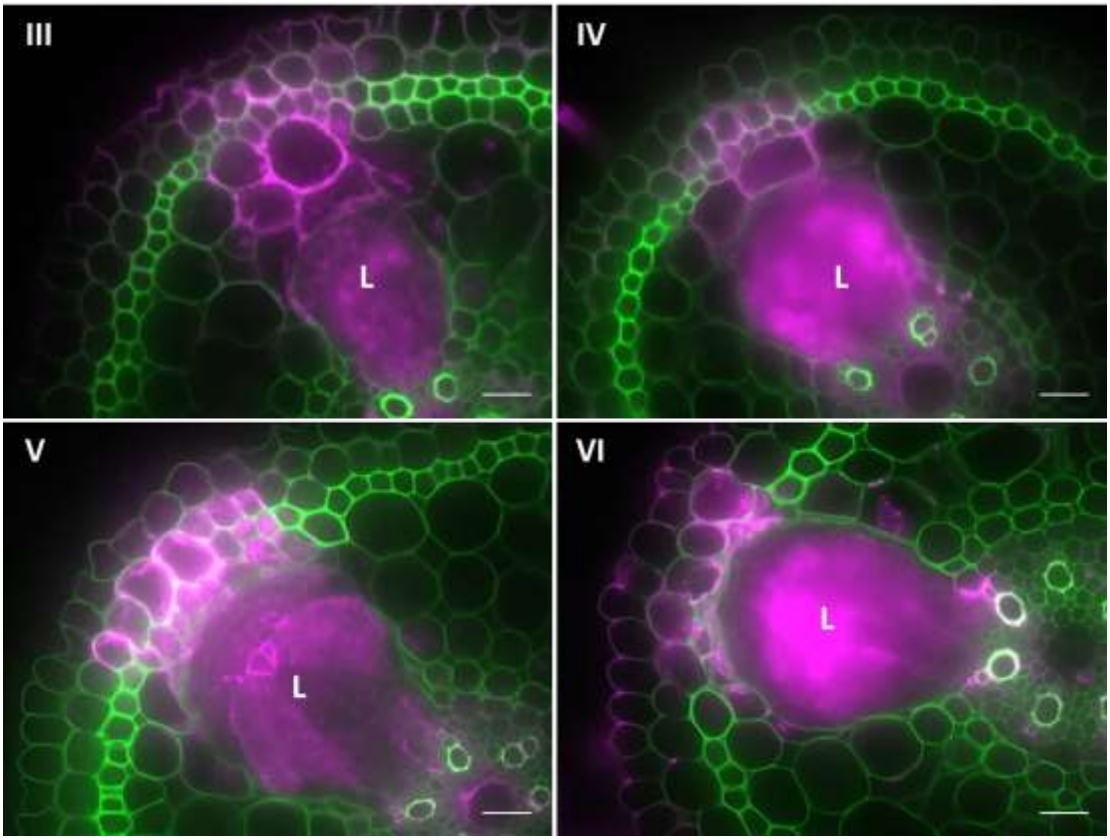

Figure 1.9 – Labeling of xyloglucan with CCRC-M100 (III-VI) Sclerenchyma and exodermis tissue overlaying the emerging lateral root primordium (L) demonstrates the presence of xyloglucan (XXXG motif) across four lateral root emergence stages in rice. Images are composite micrographs of false-colored signals from autofluorescence (green) and AlexaFluor647-conjugated secondary antibody (magenta). Bar = 20 µm.

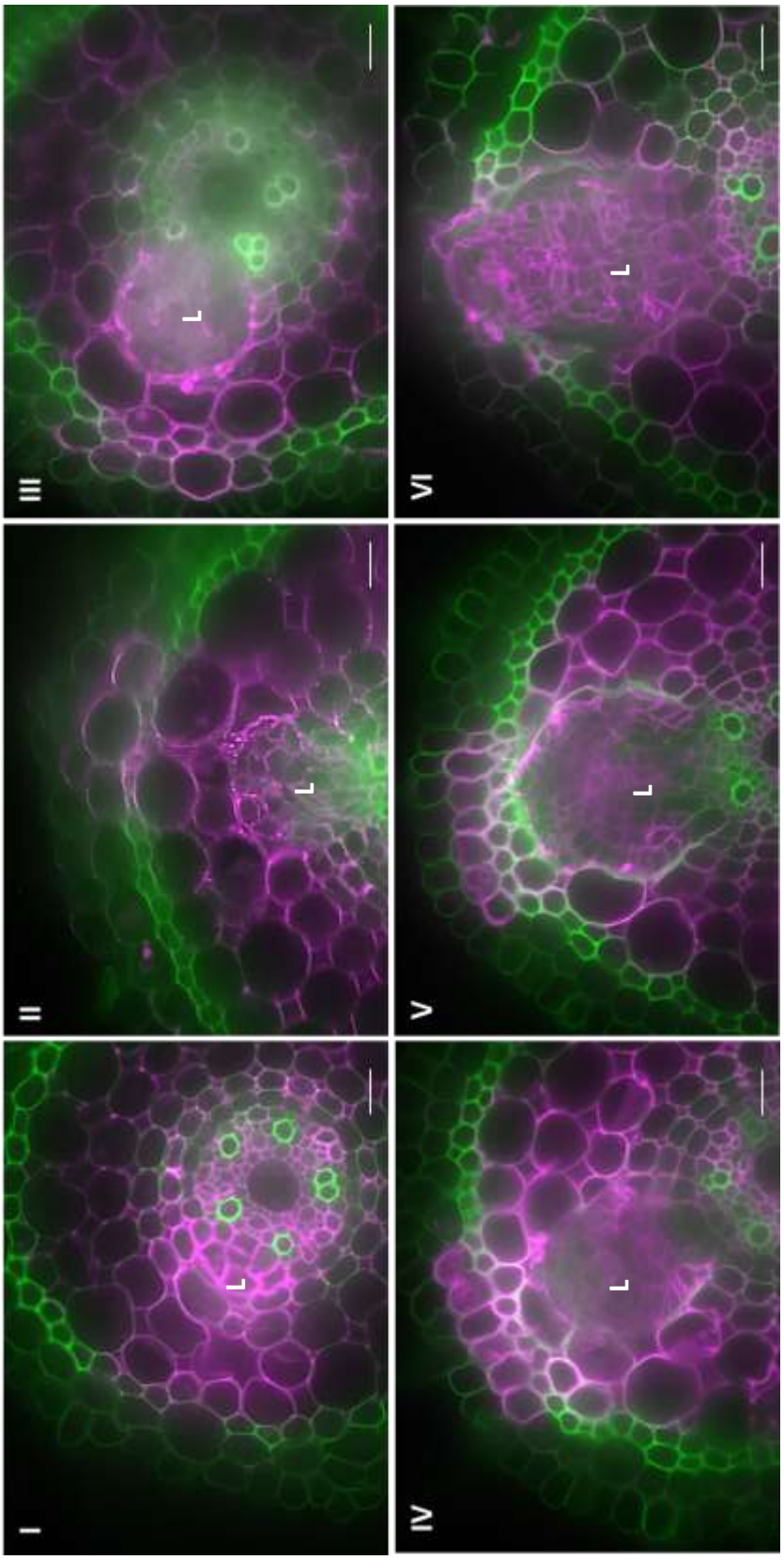
I
II
III
IV
V
VI

Figure 1.10 – Labeling of de-methyl esterified homogalacturonan with LM19 (I-VI) Sclerenchyma and exodermis tissue overlying the emerging lateral root primordium (L) demonstrate the presence of partially de-methyl esterified homogalacturonan across six lateral root emergence stages in rice. Images are composite micrographs of false-colored signals from native autofluorescence (green) and AlexaFluor647-conjugated secondary antibody (magenta). Bars = 20 µm.

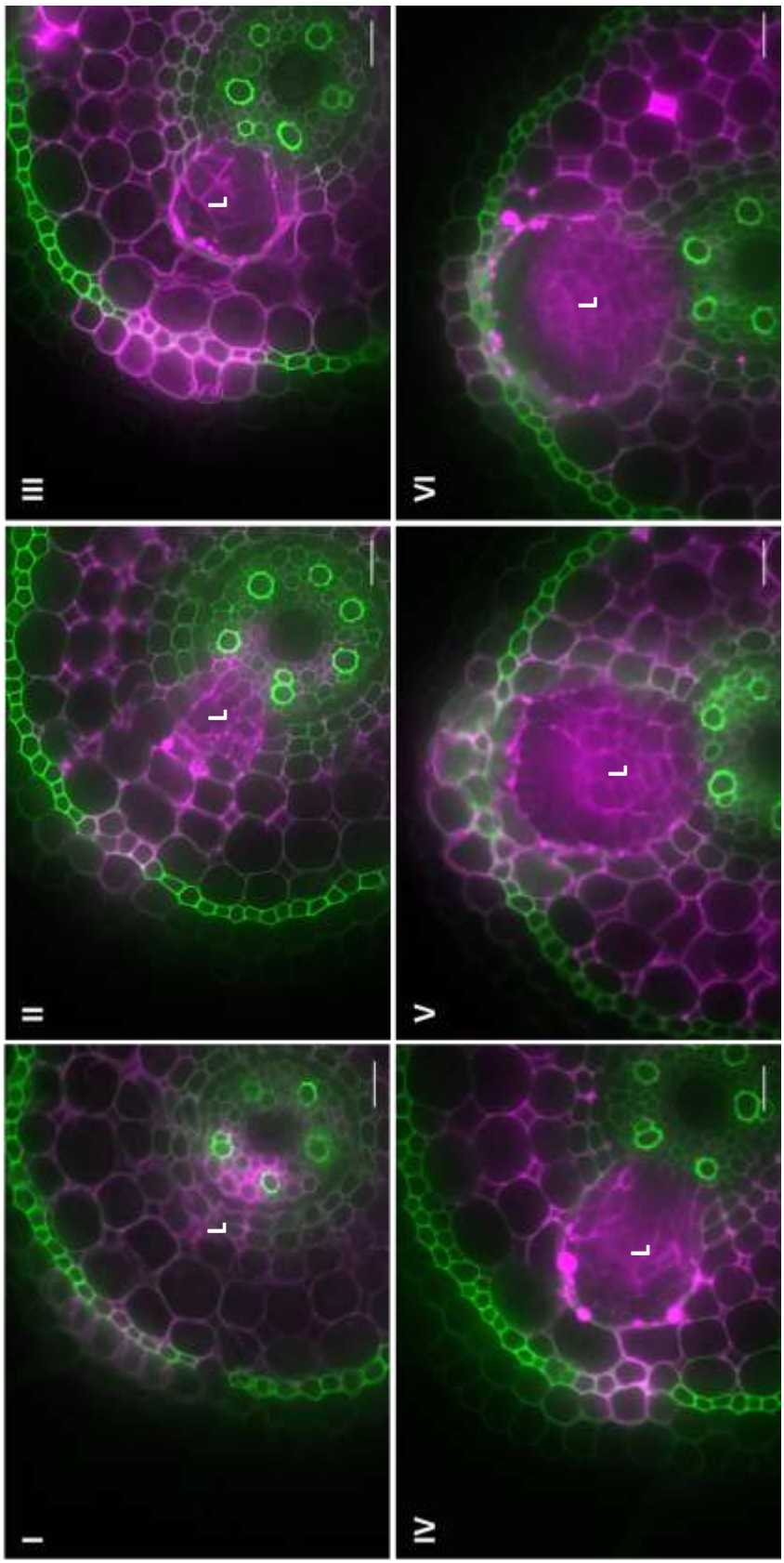
I
II
III
IV
V
VI
L

Figure 1.11 – Labeling of partially de-methyl esterified homogalacturonan with JIM5 (I-VI) Sclerenchyma and exodermis tissue overlying the emerging lateral root primordium (L) demonstrate the presence of partially de-methyl esterified homogalacturonan across six lateral root emergence stages in rice. Images are composite micrographs of false-colored signals from autofluorescence (green) and AlexaFluor647-conjugated secondary antibody (magenta). Bar = 20 µm.

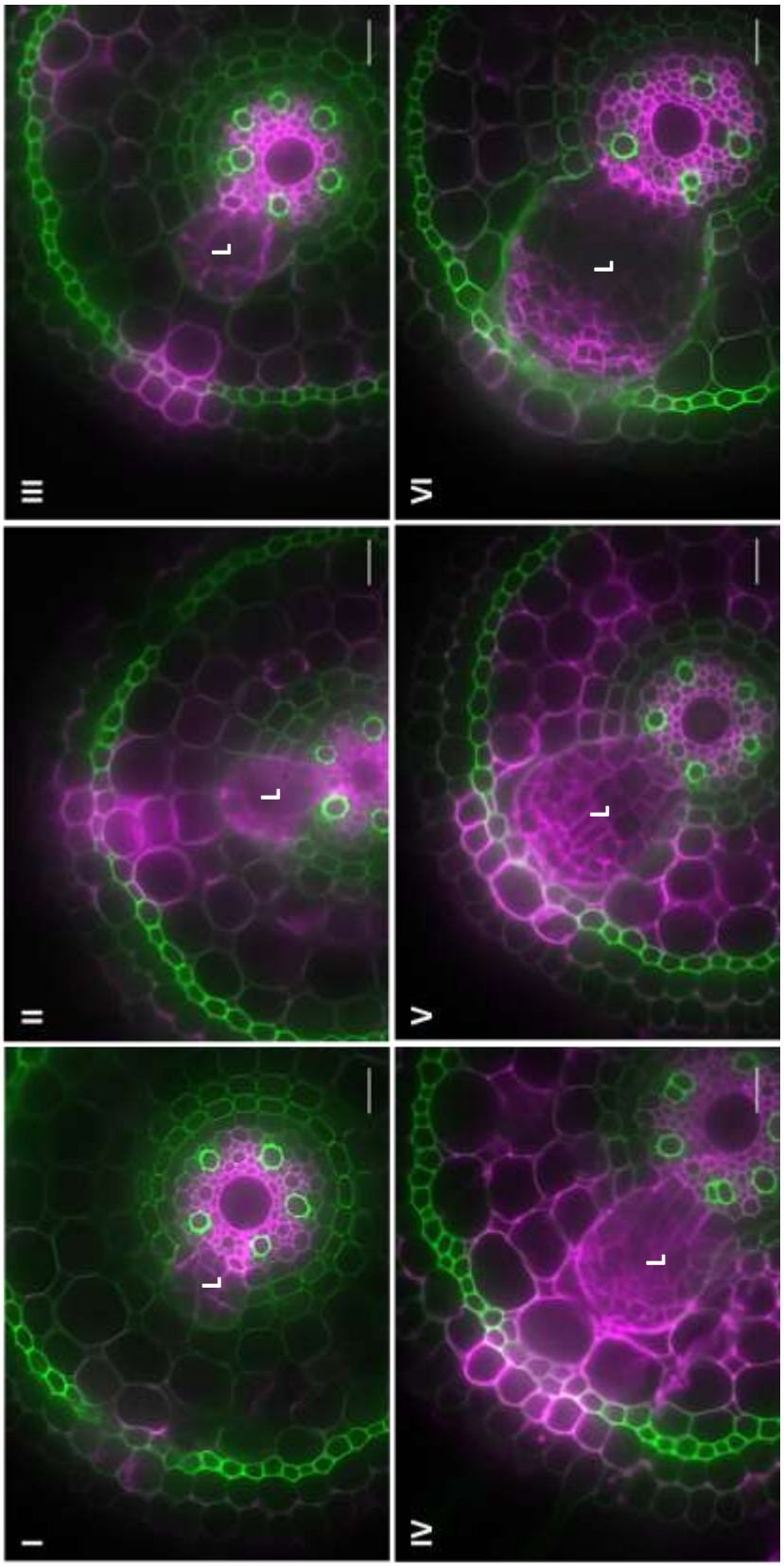
I
II
III
IV
V
VI
L

Figure 1.12 – Labeling of partially de-methyl esterified homogalacturonan with CCRC-34 (I-VI) Cortical, sclerenchyma and exodermis tissue overlying the emerging lateral root primordium (L) demonstrate the presence of partially de-methyl esterified homogalacturonan across six lateral root emergence stages in rice. Images are composite micrographs of false-colored signals from autofluorescence (green) and AlexaFluor647-conjugated secondary antibody (magenta). Bar = 20 µm.

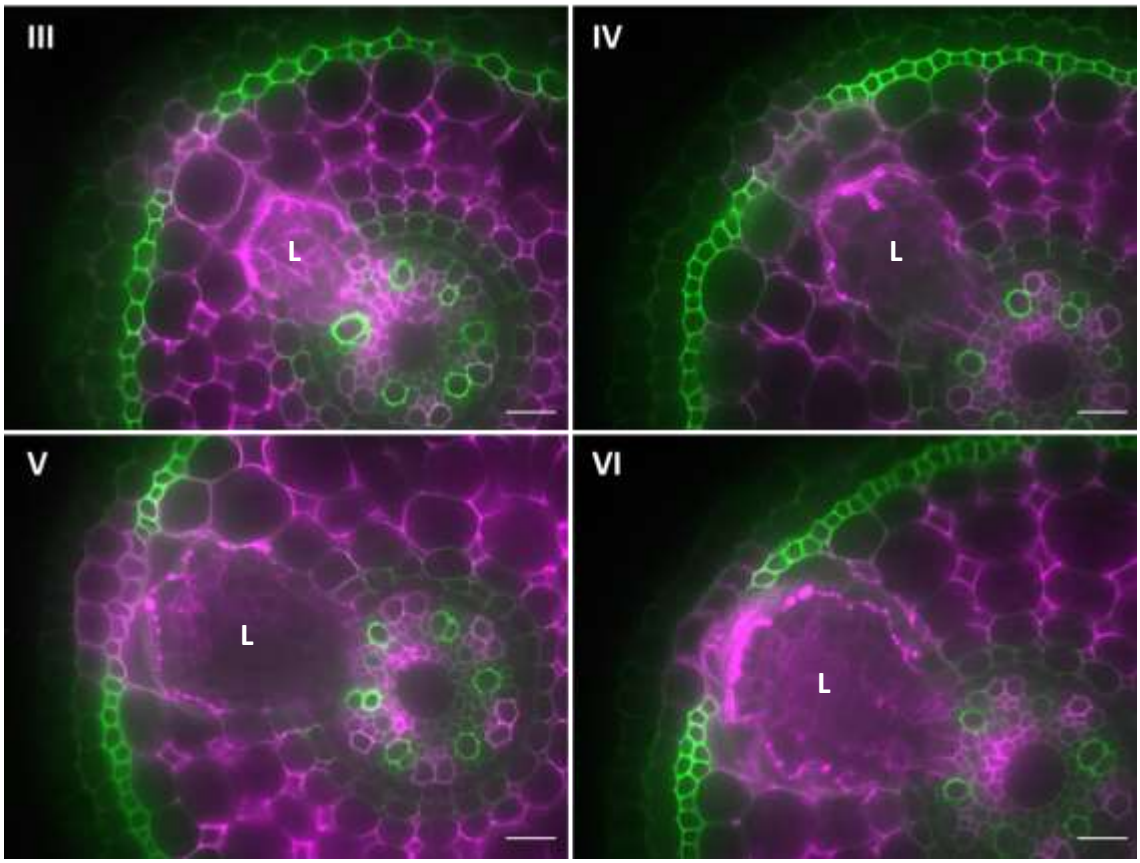

Figure 1.13 – Labeling of methyl-esterified homogalacturonan with LM20 (III-VI) Sclerenchyma and exodermis tissue overlaying the emerging lateral root primordium (L) demonstrates the presence of methyl-esterified homogalacturonan across four lateral root emergence stages in rice. Images are composite micrographs of false-colored signals from autofluorescence (green) and AlexaFluor647-conjugated secondary antibody (magenta). Bars = 20 µm.

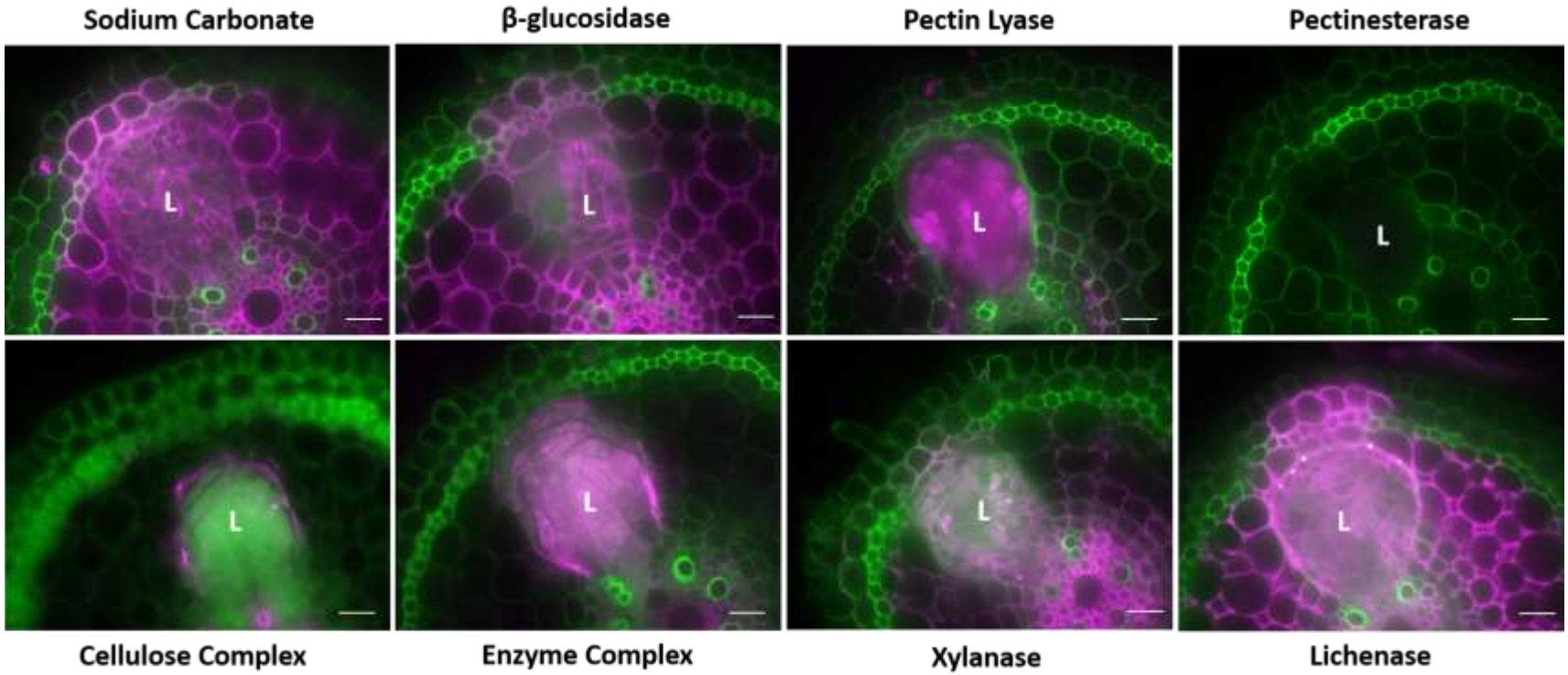
Sodium Carbonate
β-glucosidase
Pectin Lyase
Pectinesterase
L
L
L
L
L
L
L
L
Cellulose Complex
Enzyme Complex
Xylanase
Lichenase

Figure 1.14 – Impact of enzymatic treatment of rice root sections on labeling of de-methyl esterified homogalacturonan by LM19. The following enzymes were incubated with rice root cross sections prior to labelling with LM19 monoclonal antibody: cellulose complex (assorted cellulose mixture), enzyme complex (assorted cell wall degradation enzymes, negative control), xylanase, β-glucosidase, pectin lyase, pectinesterase, lichenase and sodium carbonate. Removal of LM19 binding pattern by cellulase, xylanase and pectin enzymes suggest antibody epitope is altered by removal of pectin, cellulose and hemicellulose components. Images are composite micrographs of false-colored signals from autofluorescence (green) and AlexaFluor647-conjugated secondary antibody (magenta). Bar = 20 µm.

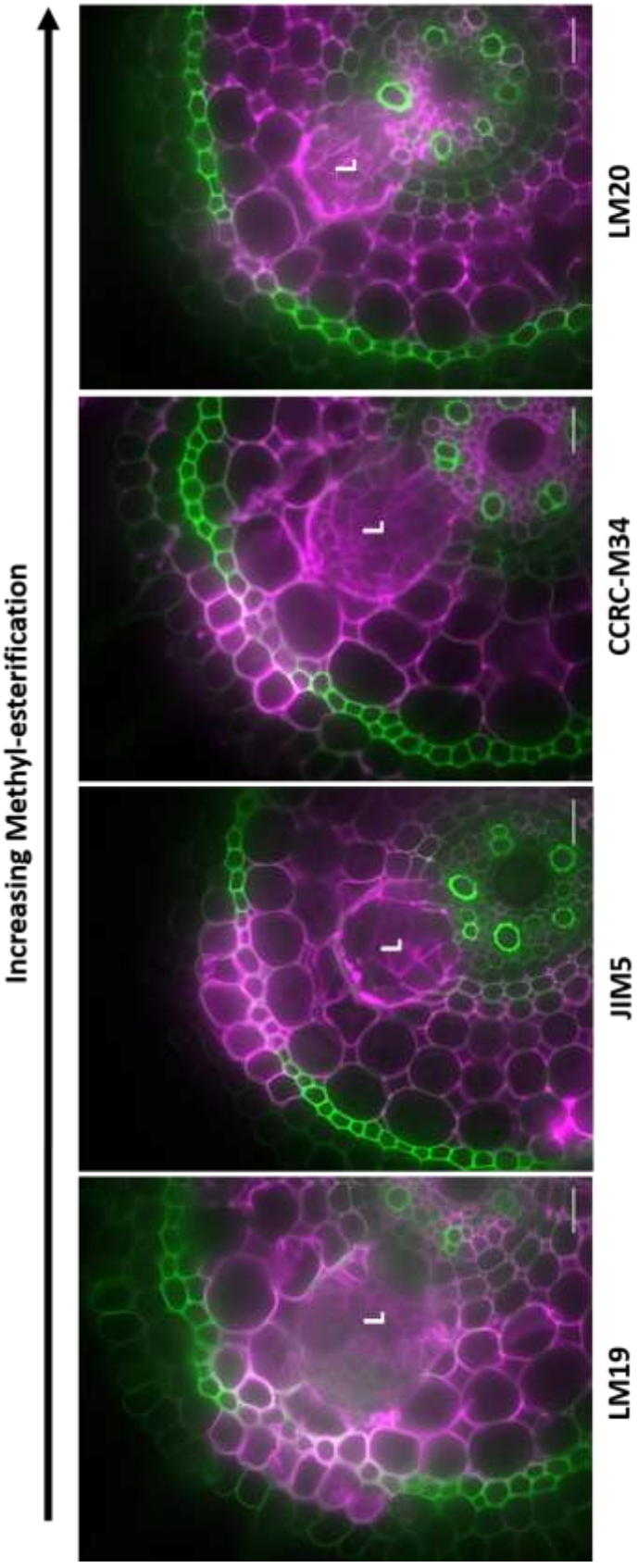
Increasing Methyl-esterification
LM19
JIM5
CCRC-M34
LM20
L
L
L
L

Figure 1.15 – Multiple degrees of methyl-esterification are present near primordia during lateral root emergence. Similar patterns of primary antibody binding in sclerenchyma and exodermis tissue overlaying the emerging lateral root primordium (L) suggests the presence of multiple methyl-esterified and de-methyl esterified homogalacturonan epitope structures during lateral root emergence in rice. Images are composite micrographs of false-colored signals from autofluorescence (green) and AlexaFluor647-conjugated secondary antibody (magenta). Bars = 20 µm.

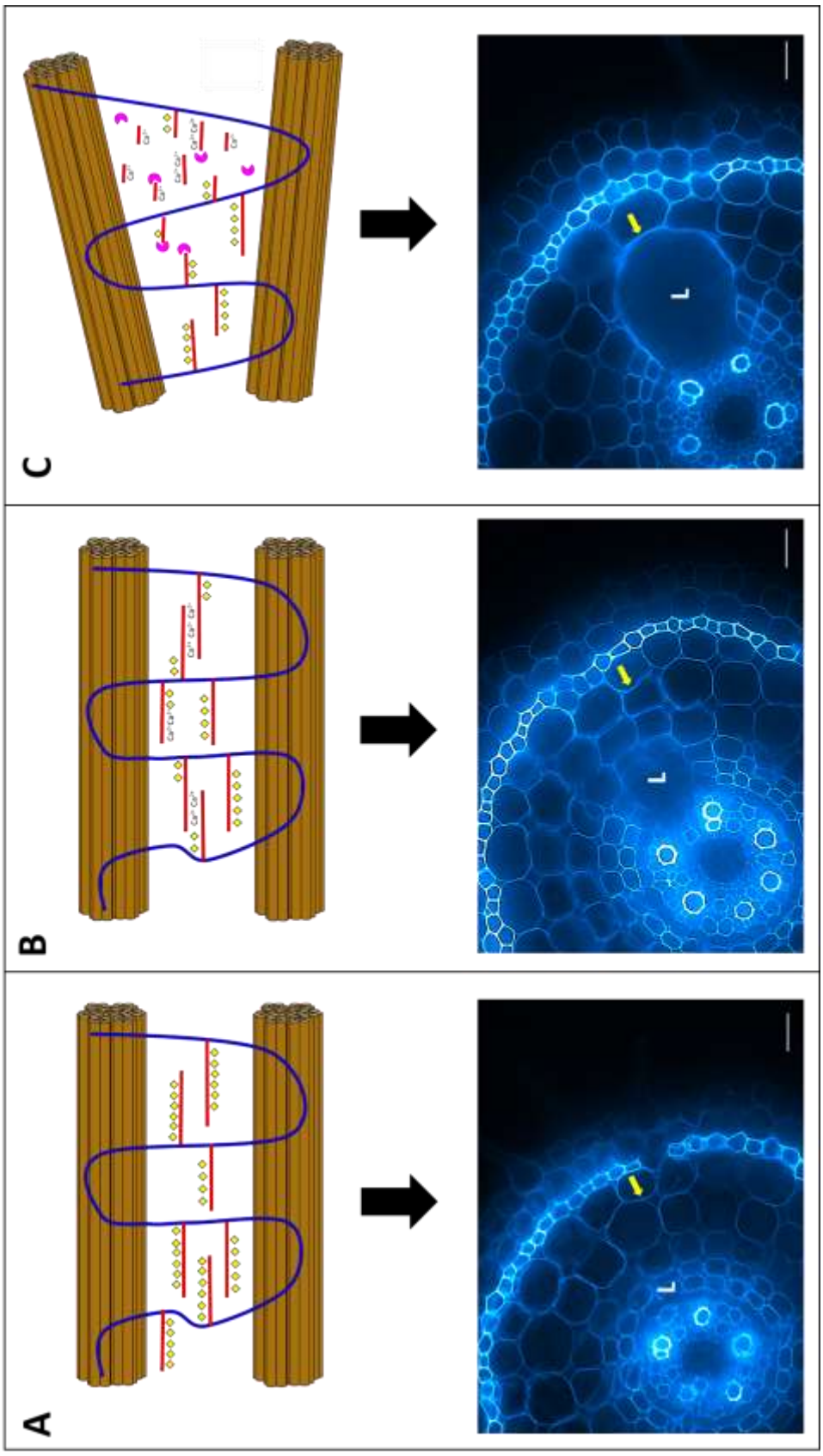
C
B
A
L
L
L

Figure 1.16 – "Loosening Model" of primary cell wall destabilization during lateral root emergence. (A) Homogalacturonan (HG) is present in primary cell walls of root tissue as a highly methyl-esterified polymer with multiple methyl groups (yellow) substituted to a D-galacturonic acid backbone (red) covalently linked to hemicellulose (blue). Before and shortly after lateral root primordia (LRP) initiation the highly methyl-esterified form of HG predominates in the primary cell walls (white arrow). (B) After de-methyl esterification occurs, calcium ions (Ca^{2+}) bind to adjacent homogalacturonan strands with exposed carboxylate ions and form an "egg-box" cross-linking structure. De-methyl esterification of the primary cell wall HG precedes the encroaching LRP. (C) Degradation of homogalacturonan backbone occurs due to polygalacturonase activity permitted by cross-linking structure. Subsequent reduction in pectin results in unstable hemicellulose structure and changes the alignment of cellulose microfibrils (brown) in the primary cell wall matrix. Weakened cell wall is distorted to accommodate primordia apex. Bar = 20 µm.

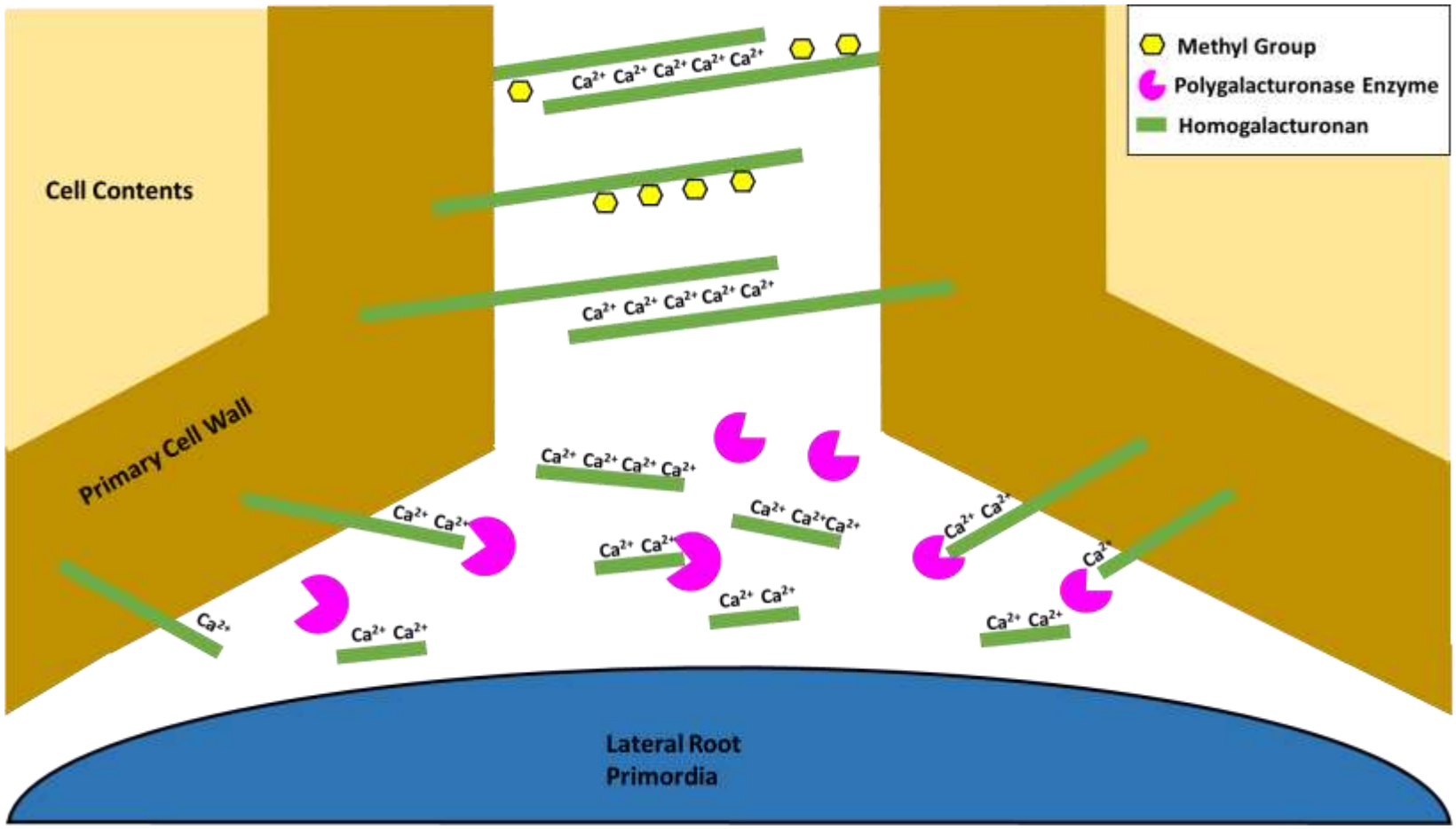
Methyl Group
Polygalacturonase Enzyme
Homogalacturonan
Cell Contents
Primary Cell Wall
Lateral Root Primordia

Figure 1.17 – "Loss of Cellular Adhesion Model" of primary cell wall destabilization during lateral root emergence. Homogalacturonan backbone (green bars) have methyl groups (yellow) removed during de-methyl esterification occurring in the middle lamella (white) between adjacent cell walls. Calcium ions (Ca^{2+}) form a complex between two or more de-methyl esterified residues on adjacent homogalacturonan chains that become susceptible to degradation by polygalacturonase (magenta). Resulting changes to the structure of the middle lamella may cause adjacent cells to be more easily separated to accommodate emerging lateral root primordia as they penetrate the root.

Chapter 2: Establishing conditions for laser-capture microdissection of tissue overlaying lateral root primordia

2-1 Background

Modification of the plant cell wall matrix is a dynamic process that often results in localized changes within plant tissues. Previous research in *Arabidopsis* suggests that primary cell wall compositional changes are highly localized in tissues adjacent to developing lateral root primordia (LRP) during lateral root emergence (Péret *et al.*, 2013). Defining the exact numbers and types of cells which experience remodeling is often visualized with histological techniques such as absorbance dye staining, immunolabeling of specific components and transmission electron microscopy of cell wall architecture. However, understanding the molecular mechanisms and gene expression behind localized cell wall remodeling requires techniques such as real-time quantitative PCR of candidate gene or whole transcriptome analysis via RNA sequencing (Chu and Corey, 2012). Sample selection for analysis of gene expression can be problematic due to small dimension, or small numbers, of cells of interest (Efroni *et al.*, 2015). For example as few as 2-3 remodeled cells per tissue layer have been observed overlaying rice LRP during various developmental stages, thereby severely limiting relevant sample areas in root cross-sections (Figure 2.1).

One technique that has been develop to harvest small quantities of tissue is laser-capture microdissection (LCM). LCM obtains very small quantities of cells from tissue sections (5-50 μm thickness) by using ultraviolet laser pulses to cut samples directly from tissues on membrane-coated glass slides, or from the tissue itself. (Espina *et al.*, 2007).

Samples of interest are then processed to extract RNA which may be prepared for RNA sequencing or converted into cDNA for other types of gene expression analysis. Another advantage of LCM lies in high-precision, automated adjustment of the cutting laser through a software interface linked to a confocal microscope, and enabling custom selection of cells of interest (Kummari *et al.*, 2015).

In the current study, limited numbers of rice root tissue cells were collected from cryopreserved cross-sections of rice roots as part of an optimized LCM harvesting protocol required for future gene expression analysis work. Understanding gene expression in highly localized areas of rice root tissues provides insight into developmental changes during lateral root emergence that may be obscured by bulk sample collection. LCM enables extremely precise tissue harvesting of several dozen, to single cells, found in a given developmental region of interest. RNA extracted from both cells localized to areas adjacent to the lateral root primordia apex, and cells on opposite sides of the rice root stele, could be utilized in RT-qPCR or transcriptome analysis to yield insight into the genetic pathway regulating the cell wall remodeling observed in lateral root emergence.

Based on the literature described in the Introduction (Kumpf *et al.*, 2013) (Péret *et al.*, 2013), and our immunofluorescent data (Figure 1.7), we expect that cells overlying emerging lateral roots will have altered expression of auxin signaling and cell wall remodeling genes (Table 1) compared to cells distal from lateral root primordia. Changes in expression during lateral root emergence would fall into two categories: up-regulated and down-regulated genes. Up-regulated genes would include auxin transporters (LAX3, PIN3) that move auxin in a controlled gradient throughout cells overlaying lateral root

primordia, and remodeling genes (PGLR, PGAZAT, EXPA17, CEL3/GH9B3 and AIR3) that either degrade major cell wall components such as homogalacturonan (PGLR and PGAZAT, polygalacturonase enzymes) and cellulose (CEL3/GH9B3, cellulase enzyme) or modify components such as cellulose microfibril linkages (EXP17, expansin protein) or the de-methyl esterification of homogalacturonan (AIR3, subtilisin-like serine protease) to destabilize/degrade the overall cell wall matrix. Down-regulated genes would include biosynthesis genes (XXT1, XEG113, and PRC1) that create hemicellulose components such as xyloglucan (XXT1) which provide strength to cell walls in the form of cellulose-xyloglucan crosslinking, modify extensins (XEG113) to promote increased cross-linking with cellulose, or synthesize cellulose microfibrils (PRC1) required to form a major part of all cell wall matrices.

2-2 Methods

Plant growth conditions and developmental staging

Developing seedlings of rice (*Oryza sativa* L. ssp. Japonica, cv. "Dongjin") were grown under fluorescent lighting in a 25^{o}C incubator. Rice was harvested from sealed petri dishes six days after initial seed germination in ½ strength Murashige and Skoog (MS) media, pH 6.5.

Root tissue harvesting and sectioning

Seedlings were harvested when six-day old plants developed 2-3 crown roots, and visible lateral roots in maturation zone tissues. Crown root sections were cut from seedlings in a sterile petri dish containing 3:1 ethanol and acetic acid fixative, under a standard dissection microscope.

LCM Harvesting & Tissue Collection

Rice root segments were immersed in 3:1 ethanol and acetic acid fixative overnight at 4^{o}C. Fixation was followed by infiltration with a graded sucrose series (10%, 15%, and 30%) for 1 hour per concentration. Samples were mounted in OCT compound (Sakura Inc.) and frozen in liquid nitrogen until solid. OCT blocks were sectioned at variable thickness (20, 40, 60 µm) on a cryostat at -22^{o}C. Approximately 20-30 sections were collected on Arcturus® PEN Membrane glass slides (Applied Biosystems) pre-chilled inside the cryostat. A minimum of 15-30 cells per rice cross section were harvested using a Zeiss Axiovert 200 confocal microscope outfitted with a P.A.L.M. Microbeam LCM nitrogen cutting laser (337 nm) to ensure adequate sample size for subsequent RNA

extraction. Samples collected with Zeiss™ AdhesiveCap 500 capture tubes and stored at -30^{o}C prior to RNA extraction.

RNA Extraction and Validation

LCM-harvested cells were lysed and purified using a NucleoSpin® RNA XS kit. RNA quantity was determine with a standard curve calculation derived from RNA standards included in a Quant-Ti™ RiboGreen® RNA Assay Kit. Nucleic acid quality was based on ratio of absorbance at 260/280 nm.

2-3 Results and Discussion

Harvesting Protocol and LCM Parameters

Optimization of laser-capture microdissection protocols, and subsequent RNA harvesting, requires several considerations in order to establish a viable protocol. Initial work focused on establishment of an initial experimental flow-through (Fig. 2.2) and systematically adjusting relevant parameters in each step prior to preparation of a cDNA library, or total RNA samples, for transcriptome analysis.

Previous research regarding LCM sample preparation suggests that cryopreservation is the preferred method for sample preparation, and permits researchers to quickly generate large quantities of preserved tissues. However, no distinct consensus exists regarding appropriate cryopreserved plant sectioning thickness for LCM application. Observation of rice root section integrity after LCM harvesting suggests that increasing section thickness yields improved morphology and ease of tissue layer identification (Figure 2.3). However, increasing thickness of tissue sections did appear to result in significant section loss during OCT-clearing protocol steps prior to LCM harvesting. Attempts to circumvent section loss by omitting OCT removal resulted in severe inhibition of tissue removal from PEN-membrane slides due to melted OCT media "gluing" the PEN membrane to the glass slide (Figure 2.4).

In addition to tissue preparation considerations, adjustment of LCM microscope setting is essential to effective harvesting of plant tissue samples. Since the coating on PEN-membrane glass slides must be removed to collect tissue samples, factors such as optimal section thickness cutting speed, cutting cycles, magnification, laser energy, and laser focus must all be evaluated to find ideal conditions (Table 3). The most crucial

setting among these results, in order of diminishing importance, are laser focus, energy and cutting speed. Laser focus narrows the ultraviolet laser of the confocal microscope onto the plane of the slide membrane, enabling sections to be excised. Laser energy is kept low to prevent scorching of the tissue sample, otherwise leading to heat-induced RNA degradation. Cutting speed must be set sufficiently high to prevent scorching, but slow enough to enable membrane excision via a low energy laser. Results indicate that optimal harvesting conditions for sclerenchyma, exodermis and epidermal tissues are found when 25 µm-thick samples are harvested under 10X magnification with laser energy 70, laser focus at 82, and cutting speed set to 1 for a minimum of five cycles (laser tracings).

RNA quantitation of LCM-harvested samples

Small samples of rice root tissue were collected from cross-sections of rice roots in order to determine the effectiveness of the optimized LCM harvesting protocol by measuring RNA quantity in excised samples. Results suggest RNA quantity per cells is similar across different rice root tissues, negating the need for different quantities of cells to be harvested per tissue layer. Preliminary results also indicated that relatively large numbers of rice root tissue cells were required to generate noticeable amounts of RNA (Table 4). Specifically, a minimum of 240 cells from either cortical tissues, or combined sclerenchyma, exodermis and epidermis tissues, was required to accumulate 9.8-14.2 ng/µL of RNA. The quantity of RNA per cell was comparable to previously recorded values in plant tissues such as tomato pericarp cells, indicating acceptable levels of RNA extraction by published standards (Matas *et al.*, 2011). Larger quantities of harvested cells

yielded greater total RNA (287.8-314.1 ng/µL), yet maintained similar quantities of RNA per cell (~ 0.1 ng/µL). Results suggest RNA quantity per cells is similar across different rice root tissues, negating the need for different quantities of cells to be harvested per tissue layer.

2-4 Conclusion

Laser capture microdissection (LCM) is a technique by which individual cells can be excised from plant tissue sections while they are viewed under a confocal microscope, by attaching selected cells to an adhesive film and dissecting the film with a laser beam. Harvested cells can then provide DNA, RNA, and protein for the profiling of genomic characteristics and transcriptome changes, gene expression, and protein spectra from individual cell types (Kerk *et al.*, 2003). LCM has tremendous application to the current study by permitting precise analysis of transcript changes in localized rice root tissue cell experiencing primary wall remodeling during lateral root emergence. Present results have yielded specific requirements for section thickness, OCT removal and microscope settings in order to optimizing LCM protocols used on rice root tissue. Results have also recommended approximate quantities of rice root cells needed for extraction of RNA similar to published standards featuring other model plants (Nakazono *et al.*, 2003).

Future studies will entail harvesting smaller quantities of rice root cells (<50) in order to evaluate the feasibility of RNA extraction from sample sizes that more accurately reflect regions of cell wall remodeling ahead of lateral root primordia. Ideally, cells from each of the eight tissue layers in the lateral root emergence pathway (endodermis, cortical cell layers 1-4, sclerenchyma, exodermis and epidermis) will be sampled and real-time, quantitative PCR (RT-qPCR) conducted to determine differences in relative expression of cell wall remodeling enzymes (polygalacturonase, cellulose, etc.) and cell wall synthesis genes (galacturonosyltransferases for pectins, galactosyltransferases for xyloglucan, etc.) between tissue layers. Furthermore, similar size samples will be harvested from tissues opposite of the rice root stele, to lateral root primordia, so a

comparison may be made between cells not experiencing alterations due to lateral root emergence, and cells in the pathway of emerging primordia

Samples harvested as previously described will also be utilized in the development of an effective T7-based RNA amplification protocol from existing literature to provide more RNA for further transcript analysis experiments (Kube *et al.*, 2007). Amplified RNA processed through an RNA sequencing (RNA-seq) platform such as Illumina (Illumina dye sequencing) will be subject to a transcriptome analysis tin order to evaluate changes in the entire range of messenger RNA (mRNA) in the rice root tissue samples. Primary focus will include transcripts for genes expressing enzymes relevant to cell wall remodeling, synthesis genes specific to known cell wall components, and genes involved in the auxin signaling pathway or auxin transport through root tissues.

A
Epidermis
Exodermis
Sclerenchyma
Cortex
Endodermis
Pericycle
B
L
C
L
D
L

Figure 2.1 – Harvesting guidelines for laser-capture microdissection. (A) Harvested tissues will either be derived from individual tissue layers, or from groups of developmental similar tissue such as the sclerenchyma-exodermis-epidermis layer constituting the outer ring of rice root cross-sections. (B) Schematic diagram of a rice root cross section with lateral root primordium (L) and tissue area of interest (pink highlight) for harvesting with laser-capture microdissection. (C) Composite micrograph displaying LM19 binding pattern for de-methyl esterified homogalacturonan (yellow) and native autofluorescence (cyan) in a lateral root primordium-containing section. (D) LCM-harvested rice root section displaying excised tissue overlaying the primordium (10X magnification).

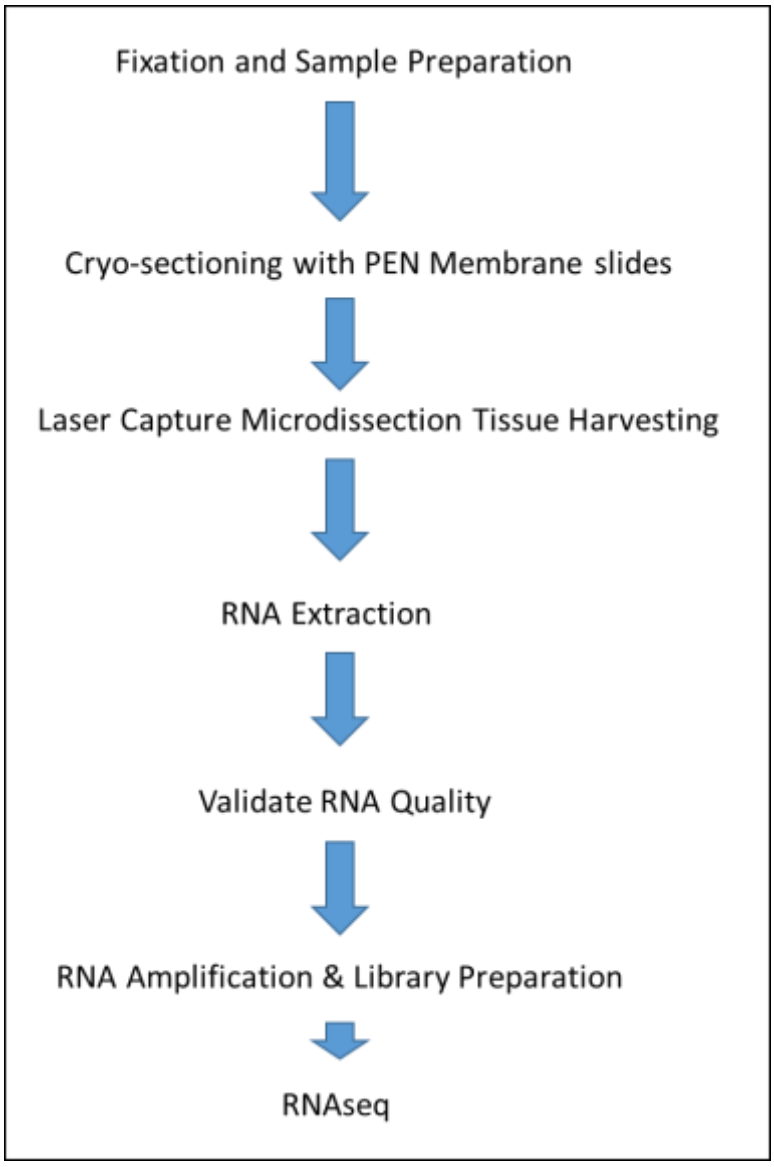

Figure 2.2 – Laser capture microdissection protocol summary. Procedure for preparing rice root tissue sections involves histological fixation and sectioning prior application of sample slices onto polymer coated PEN membrane slides. Modified confocal microscope laser enables harvesting of individual cells, which are then treated to extract total RNA. After validation of RNA quality, total RNA is amplified in preparation for cDNA library formation or transfer of samples to an RNA-seq processing facility.

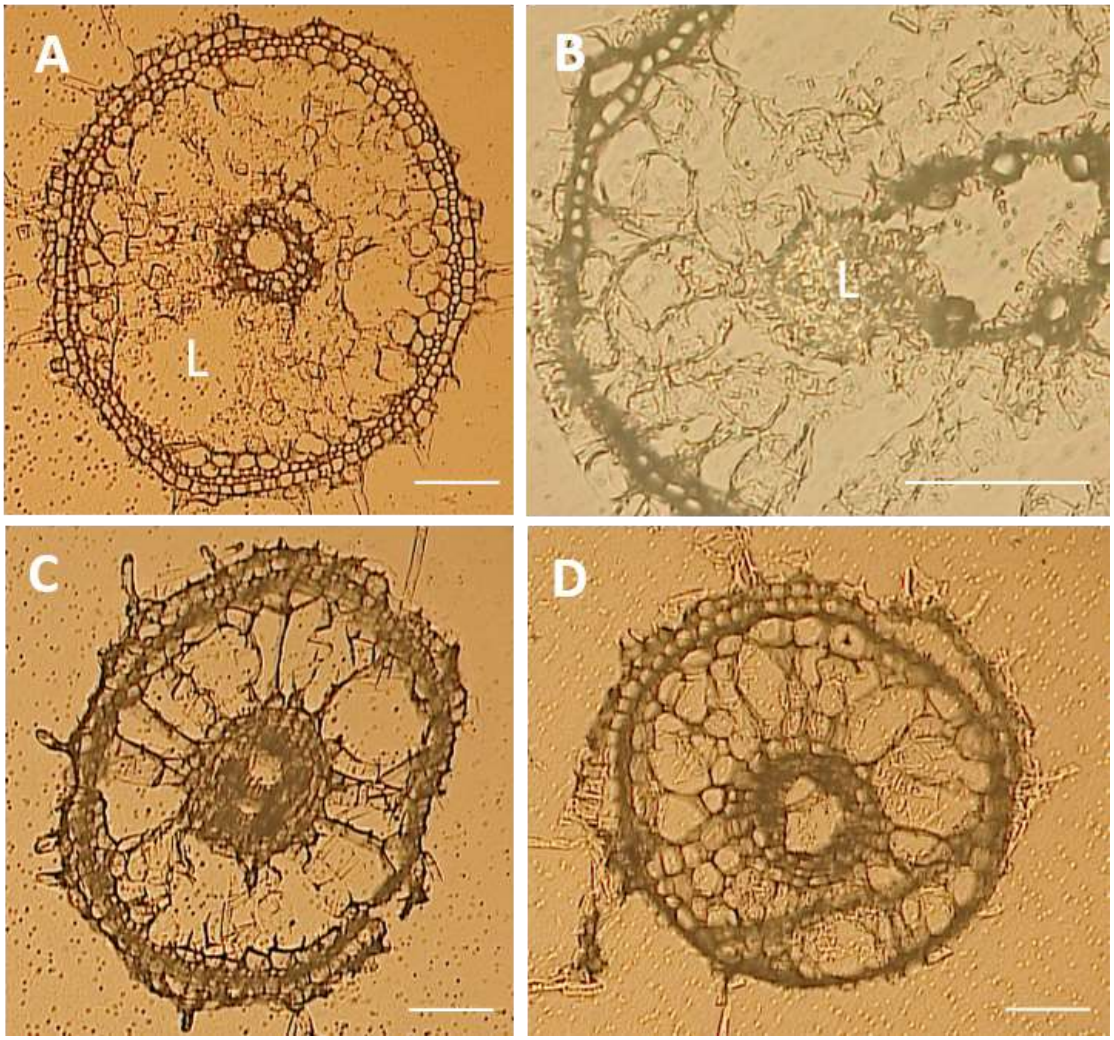

Figure 2.3 - LCM sample morphological quality impacted by section thickness (A) Rice root cross section at 14 µm thickness with lateral root primordia (L). (B) Cross section at 16 µm thickness with lateral root primordia. (C) Cross section at 20 µm thickness. (D) Cross section at 25 µm thickness. All images show sections on PEN membrane coated slides after OCT compound removal. Thicker sections demonstrate better preservation of the cortical cells, but specific tissue layers are harder to distinguish. Bright-field micrographs of all samples imaged at 10X magnification expect for (B), 40X. Bars = 50 µm.

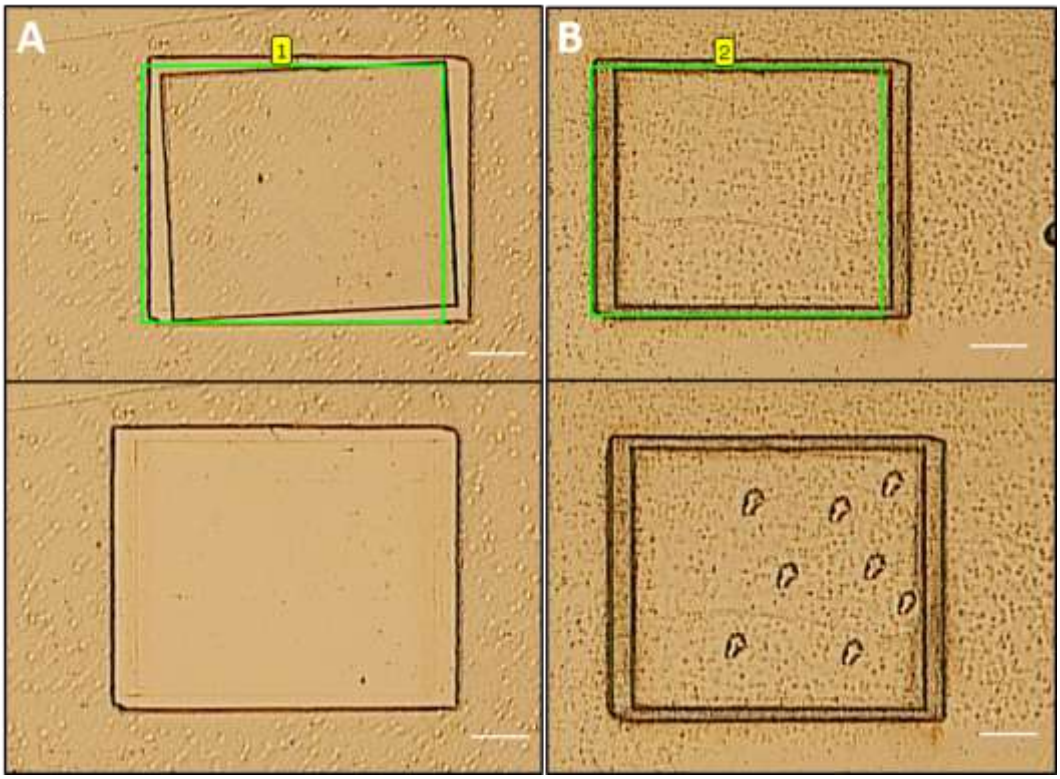

Figure 2.4 – Influence of OCT compound removal on PEN membrane excision (A) Segment of OCT-cleared PEN membrane slide before and after excision of membrane. (B) OCT-coated segment of slide before and after attempted excision. Selected membrane area (green box) failed to detach from the glass slide despite multiple confocal laser pulses. 10X magnification. Bars = 50 µm.

Table 3. Evaluation of LCM Harvesting Parameters

Section Thickness (µm)	Focus	Energy	Magnification	Cutting Cycles	Cutting Speed	Section Removal
25	82	90	10X	1	3	Yes
25	82	85	10X	3	3	Yes
25	82	75	10X	4	3	Yes
25	82	75	10X	2	3	Yes
25	82	70	10X	10	3	Yes
25	82	70	10X	6	1	Yes
25	82	70	10X	5	3	No
25	82	70	10X	5	2	No
25	82	70	10X	5	1	Yes
25	82	65	10X	18	3	No
25	82	65	10X	10	1	No
25	82	65	10X	10	2	Yes

Table 4: Relationship of LCM Cell Quantity to RNA Concentration

Tissue Type	Section Thickness (µm)	Cell Quantity	RNA Concentration (ng/µL)	RNA Concentration (ng/µL) per cell
Scl, Ex, Ep	25	1000	314.1	0.064
Cortical	25	1000	287.8	0.098
Scl., Ex, Ep.	25	500	32.11	0.17
Cortical	25	500	49.075	0.17
Scl., Ex, Ep.	25	240	14.2	0.03
Cortical.	25	240	13.3	0.04
Scl., Ex, Ep.	25	240	9.8	0.03
Cortical	25	240	11.0	0.04

* Scl = Sclerenchyma, Ex = Exodermis, Ep = Epidermis

References

Aalen RB, Wildhagen M, Stø IM, Butenko MA. 2013. IDA: a peptide ligand regulating cell separation processes in Arabidopsis. *Journal of Experimental Botany* **64**, 5253-5261.

Abasolo W, Eder M, Yamauchi K, Obel N, Reinecke A, Neumetzler L, Dunlop JWC, Mouille G, Pauly M, Höfte H, Burgert I. 2009. Pectin May Hinder the Unfolding of Xyloglucan Chains during Cell Deformation: Implications of the Mechanical Performance of Arabidopsis Hypocotyls with Pectin Alterations. *Molecular Plant* **2**, 990-999.

Agustí J, Merelo P, Cercós M, Tadeo FR, Talón M. 2009. Comparative transcriptional survey between laser-microdissected cells from laminar abscission zone and petiolar cortical tissue during ethylene-promoted abscission in citrus leaves. *BMC Plant Biology* **9**, 127-127.

Arancibia RA, Motsenbocker CE. 2006. Pectin methylesterase activity in vivo differs from activity in vitro and enhances polygalacturonase-mediated pectin degradation in tabasco pepper. *Journal of Plant Physiology* **163**, 488-496.

Atkinson JA, Rasmussen A, Traini R, Voß U, Sturrock C, Mooney SJ, Wells DM, Bennett MJ. 2014. Branching Out in Roots: Uncovering Form, Function, and Regulation. *Plant Physiology* **166**, 538-550.

Bhalerao RP, Eklöf J, Ljung K, Marchant A, Bennett M, Sandberg G. 2002. Shoot-derived auxin is essential for early lateral root emergence in Arabidopsis seedlings. *The Plant Journal* **29**, 325-332.

Braccini I, Pérez S. 2001. Molecular Basis of Ca2+-Induced Gelation in Alginates and Pectins: The Egg-Box Model Revisited. *Biomacromolecules* **2**, 1089-1096.

Butenko MA, Patterson SE, Grini PE, Stenvik G-E, Amundsen SS, Mandal A, Aalen RB. 2003. INFLORESCENCE DEFICIENT IN ABSCISSION Controls Floral Organ Abscission in Arabidopsis and Identifies a Novel Family of Putative Ligands in Plants. *The Plant Cell* **15**, 2296-2307.

Caffall KH, Mohnen D. 2009. The structure, function, and biosynthesis of plant cell wall pectic polysaccharides. *Carbohydrate Research* **344**, 1879-1900.

Carpita NC. 1996. STRUCTURE AND BIOGENESIS OF THE CELL WALLS OF GRASSES. *Annual Review of Plant Physiology and Plant Molecular Biology* **47**, 445-476.

Carpita NC, Gibeaut DM. 1993. Structural models of primary cell walls in flowering plants: consistency of molecular structure with the physical properties of the walls during growth. *The Plant Journal* **3**, 1-30.

Cavalier DM, Lerouxel O, Neumetzler L, Yamauchi K, Reinecke A, Freshour G, Zabotina OA, Hahn MG, Burgert I, Pauly M, Raikhel NV, Keegstra K. 2008. Disrupting Two Arabidopsis thaliana Xylosyltransferase Genes Results in Plants Deficient in Xyloglucan, a Major Primary Cell Wall Component. *The Plant Cell* **20**, 1519-1537.

Chen X, Vega-Sánchez ME, Verhertbruggen Y, Chiniquy D, Canlas PE, Fagerström A, Prak L, Christensen U, Oikawa A, Chern M, Zuo S, Lin F, Auer M, Willats WGT, Bartley L, Harholt J, Scheller HV, Ronald PC. Inactivation of OsIRX10 Leads to Decreased Xylan Content in Rice Culm Cell Walls and Improved Biomass Saccharification. *Molecular Plant* **6**, 570-573.

Christiansen LC, Dal Degan F, Ulvskov P, Borkhardt B. 2002. Examination of the dehiscence zone in soybean pods and isolation of a dehiscence-related endopolygalacturonase gene. *Plant, Cell & Environment* **25**, 479-490.

Chu Y, Corey DR. 2012. RNA Sequencing: Platform Selection, Experimental Design, and Data Interpretation. *Nucleic Acid Therapeutics* **22**, 271-274.

Clark N, De Luis Balaguer MA, Sozzani R. 2014. Experimental data and computational modeling link auxin gradient and development in the Arabidopsis root. *Frontiers in Plant Science* **5**.

Cosgrove D, Jarvis m. 2012. Comparative structure and biomechanics of plant primary and secondary cell walls. *Frontiers in Plant Science* **3**.

Cosgrove DJ. 2005. Growth of the plant cell wall. *Nat Rev Mol Cell Biol* **6**, 850-861.

De Rybel B, Audenaert D, Xuan W, Overvoorde P, Strader LC, Kepinski S, Hoye R, Brisbois R, Parizot B, Vanneste S, Liu X, Gilday A, Graham IA, Nguyen L, Jansen L, Njo MF, Inzé D, Bartel B, Beeckman T. 2012. A role for the root cap in root branching revealed by the non-auxin probe naxillin. *Nat Chem Biol* **8**, 798-805.
De Rybel B, Vassileva V, Parizot B, Demeulenaere M, Grunewald W, Audenaert D, Van Campenhout J, Overvoorde P, Jansen L, Vanneste S, Möller B, Wilson M, Holman T, Van Isterdael G, Brunoud G, Vuylsteke M, Vernoux T, De Veylder L, Inzé D, Weijers D, Bennett MJ, Beeckman T. 2010. A Novel Aux/IAA28 Signaling Cascade Activates GATA23-Dependent Specification of Lateral Root Founder Cell Identity. *Current Biology* **20**, 1697-1706.

De Smet I. 2012. Lateral root initiation: one step at a time. *New Phytologist* **193**, 867-873.

De Smet I, Tetsumura T, De Rybel B, Frey NFd, Laplaze L, Casimiro I, Swarup R, Naudts M, Vanneste S, Audenaert D, Inzé D, Bennett MJ, Beeckman T. 2007. Auxin-dependent regulation of lateral root positioning in the basal meristem of Arabidopsis. *Development* **134**, 681-690.

dos Santos CR, Cordeiro RL, Wong DWS, Murakami MT. 2015. Structural Basis for Xyloglucan Specificity and α-d-Xylp(1 → 6)-d-Glcp Recognition at the −1 Subsite within the GH5 Family. *Biochemistry* **54**, 1930-1942.

Dubrovsky JG, Doerner PW, Colón-Carmona A, Rost TL. 2000. Pericycle Cell Proliferation and Lateral Root Initiation in Arabidopsis. *Plant Physiology* **124**, 1648-1657.

Dubrovsky JG, Rost TL, Colón-Carmona A, Doerner P. 2001. Early primordium morphogenesis during lateral root initiation in Arabidopsis thaliana. *Planta* **214**, 30-36.

Efroni I, Ip P-L, Nawy T, Mello A, Birnbaum KD. 2015. Quantification of cell identity from single-cell gene expression profiles. *Genome Biology* **16**, 1-12.

Espina V, Heiby M, Pierobon M, Liotta LA. 2007. Laser capture microdissection technology. *Expert Review of Molecular Diagnostics* **7**, 647-657.

Fagard M, Desnos T, Desprez T, Goubet F, Refregier G, Mouille G, McCann M, Rayon C, Vernhettes S, Höfte H. 2000. PROCUSTE1 Encodes a Cellulose Synthase Required for Normal Cell Elongation Specifically in Roots and Dark-Grown Hypocotyls of Arabidopsis. *The Plant Cell* **12**, 2409-2423.

Fendrych M, Van Hautegem T, Van Durme M, Olvera-Carrillo Y, Huysmans M, Karimi M, Lippens S, Guérin Christopher J, Krebs M, Schumacher K, Nowack Moritz K. 2014. Programmed Cell Death Controlled by ANAC033/SOMBRERO Determines Root Cap Organ Size in Arabidopsis. *Current Biology* **24**, 931-940.

Goulao LF, Oliveira CM. 2008. Cell wall modifications during fruit ripening: when a fruit is not the fruit. *Trends in Food Science & Technology* **19**, 4-25.

Harris PJ, Hartley RD. 1976. Detection of bound ferulic acid in cell walls of the Gramineae by ultraviolet fluorescence microscopy. *Nature* **259**, 508-510.

Henry S, Divol F, Bettembourg M, Bureau C, Guiderdoni E, Perin C, Dievart A. 2016. Immunoprofiling of rice root cortex reveals two cortical subdomains. *Frontiers in Plant Science* **6**.

Hervé C, Marcus SE, Knox JP. 2011. Monoclonal Antibodies, Carbohydrate-Binding Modules, and the Detection of Polysaccharides in Plant Cell Walls. In: Popper AZ, ed. *The Plant Cell Wall: Methods and Protocols*. Totowa, NJ: Humana Press, 103-113.

Hochholdinger F, Zimmermann R. 2008. Conserved and diverse mechanisms in root development. *Current Opinion in Plant Biology* **11**, 70-74.

Iain EPT, Julia CW, Alex LM, Frank V. 1990. Use of Chemical Fractionation and Proton Nuclear Magnetic Resonance to Probe the Physical Structure of the Primary Plant Cell Wall. *Plant Physiology* **94**, 174-178.

Itoh J-I, Nonomura K-I, Ikeda K, Yamaki S, Inukai Y, Yamagishi H, Kitano H, Nagato Y. 2005. Rice Plant Development: from Zygote to Spikelet. *Plant and Cell Physiology* **46**, 23-47.

Jia YJ, Feng BZ, Sun WX, Zhang XG. 2009. Polygalacturonase, Pectate Lyase and Pectin Methylesterase Activity in Pathogenic Strains of Phytophthora capsici Incubated under Different Conditions. *Journal of Phytopathology* **157**, 585-591.

Kader MA, Lindberg S. 2010. Cytosolic calcium and pH signaling in plants under salinity stress. *Plant Signaling & Behavior* **5**, 233-238.

Kerk NM, Ceserani T, Tausta SL, Sussex IM, Nelson TM. 2003. Laser Capture Microdissection of Cells from Plant Tissues. *Plant Physiology* **132**, 27-35.

Kube DM, Savci-Heijink CD, Lamblin A-F, Kosari F, Vasmatzis G, Cheville JC, Connelly DP, Klee GG. 2007. Optimization of laser capture microdissection and RNA amplification for gene expression profiling of prostate cancer. *BMC Molecular Biology* **8**, 1-14.

Kummari E, Guo-Ross SX, Eells JB. 2015. Laser Capture Microdissection - A Demonstration of the Isolation of Individual Dopamine Neurons and the Entire Ventral Tegmental Area. *Journal of Visualized Experiments : JoVE*, 52336.

Kumpf RP, Shi C-L, Larrieu A, Stø IM, Butenko MA, Péret B, Riiser ES, Bennett MJ, Aalen RB. 2013. Floral organ abscission peptide IDA and its HAE/HSL2 receptors control cell separation during lateral root emergence. *Proceedings of the National Academy of Sciences* **110**, 5235-5240.

Lewis DR, Olex AL, Lundy SR, Turkett WH, Fetrow JS, Muday GK. 2013. A Kinetic Analysis of the Auxin Transcriptome Reveals Cell Wall Remodeling Proteins That Modulate Lateral Root Development in Arabidopsis. *The Plant Cell* **25**, 3329-3346.

Ljung K, Hull AK, Celenza J, Yamada M, Estelle M, Normanly J, Sandberg G. 2005. Sites and Regulation of Auxin Biosynthesis in Arabidopsis Roots. *The Plant Cell* **17**, 1090-1104.

Matas AJ, Yeats TH, Buda GJ, Zheng Y, Chatterjee S, Tohge T, Ponnala L, Adato A, Aharoni A, Stark R, Fernie AR, Fei Z, Giovannoni JJ, Rose JKC. 2011. Tissue-

and Cell-Type Specific Transcriptome Profiling of Expanding Tomato Fruit Provides Insights into Metabolic and Regulatory Specialization and Cuticle Formation. *The Plant Cell* **23**, 3893-3910.

Mohnen D. 2008. Pectin structure and biosynthesis. *Current Opinion in Plant Biology* **11**, 266-277.

Nakazono M, Qiu F, Borsuk LA, Schnable PS. 2003. Laser-Capture Microdissection, a Tool for the Global Analysis of Gene Expression in Specific Plant Cell Types: Identification of Genes Expressed Differentially in Epidermal Cells or Vascular Tissues of Maize. *The Plant Cell* **15**, 583-596.

O'Neill MA, Ishii T, Albersheim P, Darvill AG. 2004. RHAMNOGALACTURONAN II: Structure and Function of a Borate Cross-Linked Cell Wall Pectic Polysaccharide. *Annual Review of Plant Biology* **55**, 109-139.

Ochoa-Villarreal M, Aispuro-Hernández E, Martínez-Téllez MA, Vargas-Arispuro I. 2012. *Plant Cell Wall Polymers: Function, Structure and Biological Activity of Their Derivatives*.

Overvoorde P, Fukaki H, Beeckman T. 2010. Auxin Control of Root Development. *Cold Spring Harbor Perspectives in Biology* **2**, a001537.

Paque S, Mouille G, Grandont L, Alabadí D, Gaertner C, Goyallon A, Muller P, Primard-Brisset C, Sormani R, Blázquez MA, Perrot-Rechenmann C. 2014. AUXIN BINDING PROTEIN1 Links Cell Wall Remodeling, Auxin Signaling, and Cell Expansion in Arabidopsis. *The Plant Cell Online*.

Pattathil S, Hahn MG, Dale BE, Chundawat SPS. 2015. Insights into plant cell wall structure, architecture, and integrity using glycome profiling of native and AFEXTM-pre-treated biomass. *Journal of Experimental Botany* **66**, 4279-4294.

Pauly M, Albersheim P, Darvill A, York WS. 1999. Molecular domains of the cellulose/xyloglucan network in the cell walls of higher plants. *The Plant Journal* **20**, 629-639.

Péret B, Larrieu A, Bennett MJ. 2009. Lateral root emergence: a difficult birth. *Journal of Experimental Botany* **60**, 3637-3643.

Péret B, Middleton AM, French AP, Larrieu A, Bishopp A, Njo M, Wells DM, Porco S, Mellor N, Band LR, Casimiro I, Kleine-Vehn J, Vanneste S, Sairanen I, Mallet R, Sandberg G, Ljung K, Beeckman T, Benkova E, Friml J, Kramer E, King JR, De Smet I, Pridmore T, Owen M, Bennett MJ. 2013. Sequential induction of auxin efflux and influx carriers regulates lateral root emergence. *Molecular Systems Biology* **9**, 699-699.

Péret B, Swarup K, Ferguson A, Seth M, Yang Y, Dhondt S, James N, Casimiro I, Perry P, Syed A, Yang H, Reemmer J, Venison E, Howells C, Perez-Amador MA, Yun J, Alonso J, Beemster GTS, Laplaze L, Murphy A, Bennett MJ, Nielsen E, Swarup R. 2012. AUX/LAX Genes Encode a Family of Auxin Influx Transporters That Perform Distinct Functions during Arabidopsis Development. *The Plant Cell* **24**, 2874-2885.

Petrášek J, Friml J. 2009. Auxin transport routes in plant development. *Development* **136**, 2675-2688.

Plazinski W. 2011. Molecular basis of calcium binding by polyguluronate chains. Revising the egg-box model. *Journal of Computational Chemistry* **32**, 2988-2995.

Rafińska K, Świdziński M, Bednarska-Kozakiewicz E. 2014. Homogalacturonan deesterification during pollen–ovule interaction in Larix decidua Mill.: an immunocytochemical study. *Planta* **240**, 195-208.

Ridley BL, O'Neill MA, Mohnen D. 2001. Pectins: structure, biosynthesis, and oligogalacturonide-related signaling. *Phytochemistry* **57**, 929-967.

Robert HS, Friml J. 2009. Auxin and other signals on the move in plants. *Nat Chem Biol* **5**, 325-332.

Roycewicz PS, Malamy JE. 2014. Cell wall properties play an important role in the emergence of lateral root primordia from the parent root. *Journal of Experimental Botany* **65**, 2057-2069.

Sato A, Miura K. 2011. Root architecture remodeling induced by phosphate starvation. *Plant Signaling & Behavior* **6**, 1122-1126.

Sato Y, Antonio BA, Namiki N, Takehisa H, Minami H, Kamatsuki K, Sugimoto K, Shimizu Y, Hirochika H, Nagamura Y. 2010. RiceXPro: a platform for monitoring gene expression in japonica rice grown under natural field conditions. *Nucleic Acids Research*.

Scheller HV, Jensen JK, Sørensen SO, Harholt J, Geshi N. 2007. Biosynthesis of pectin. *Physiologia Plantarum* **129**, 283-295.

Smith S, De Smet I. 2012. Root system architecture: insights from Arabidopsis and cereal crops. *Philosophical Transactions of the Royal Society B: Biological Sciences* **367**, 1441-1452.

Swarup K, Benkova E, Swarup R, Casimiro I, Peret B, Yang Y, Parry G, Nielsen E, De Smet I, Vanneste S, Levesque MP, Carrier D, James N, Calvo V, Ljung K, Kramer E, Roberts R, Graham N, Marillonnet S, Patel K, Jones JDG, Taylor CG, Schachtman DP, May S, Sandberg G, Benfey P, Friml J, Kerr I, Beeckman T,

Laplaze L, Bennett MJ. 2008. The auxin influx carrier LAX3 promotes lateral root emergence. *Nat Cell Biol* **10**, 946-954.

Tenhaken R. 2014. Cell wall remodeling under abiotic stress. *Frontiers in Plant Science* **5**, 771.

Teugjas H, Väljamäe P. 2013. Selecting β-glucosidases to support cellulases in cellulose saccharification. *Biotechnology for Biofuels* **6**, 1-13.

Tian H, De Smet I, Ding Z. 2014. Shaping a root system: regulating lateral versus primary root growth. *Trends in Plant Science* **19**, 426-431.

Tranquet O, Saulnier L, Utille J-P, Ralph J, Guillon F. 2009. Monoclonal antibodies to p-coumarate. *Phytochemistry* **70**, 1366-1373.

van der Weijde T, Alvim Kamei CL, Torres AF, Vermerris W, Dolstra O, Visser RGF, Trindade LM. 2013. The potential of C4 grasses for cellulosic biofuel production. *Frontiers in Plant Science* **4**, 107.

Vanholme R, Demedts B, Morreel K, Ralph J, Boerjan W. 2010. Lignin Biosynthesis and Structure. *Plant Physiology* **153**, 895-905.

Vega-Sánchez ME, Verhertbruggen Y, Scheller HV, Ronald PC. 2013. Abundance of mixed linkage glucan in mature tissues and secondary cell walls of grasses. *Plant Signaling & Behavior* **8**, e23143.

Vermeer JEM, von Wangenheim D, Barberon M, Lee Y, Stelzer EHK, Maizel A, Geldner N. 2014. A Spatial Accommodation by Neighboring Cells Is Required for Organ Initiation in Arabidopsis. *Science* **343**, 178-183.

Vilches-Barro A, Maizel A. 2015. Talking through walls: mechanisms of lateral root emergence in Arabidopsis thaliana. *Current Opinion in Plant Biology* **23**, 31-38.

Vogel J. 2008. Unique aspects of the grass cell wall. *Current Opinion in Plant Biology* **11**, 301-307.

Wakabayashi K, Hoson T, Huber DJ. 2003. Methyl de-esterification as a major factor regulating the extent of pectin depolymerization during fruit ripening: a comparison of the action of avocado (Persea americana) and tomato (Lycopersicon esculentum) polygalacturonases. *Journal of Plant Physiology* **160**, 667-673.

Willats WGT, Knox JP, Mikkelsen JD. 2006. Pectin: new insights into an old polymer are starting to gel. *Trends in Food Science & Technology* **17**, 97-104.

Willats WGT, Orfila C, Limberg G, Buchholt HC, van Alebeek G-JWM, Voragen AGJ, Marcus SE, Christensen TMIE, Mikkelsen JD, Murray BS, Knox JP. 2001.

Modulation of the Degree and Pattern of Methyl-esterification of Pectic Homogalacturonan in Plant Cell Walls: IMPLICATIONS FOR PECTIN METHYL ESTERASE ACTION, MATRIX PROPERTIES, AND CELL ADHESION. *Journal of Biological Chemistry* **276**, 19404-19413.

Wolf S, Mouille G, Pelloux J. 2009. Homogalacturonan Methyl-Esterification and Plant Development. *Molecular Plant* **2**, 851-860.

Xuan W, Band LR, Kumpf RP, Van Damme D, Parizot B, De Rop G, Opdenacker D, Möller BK, Skorzinski N, Njo MF, De Rybel B, Audenaert D, Nowack MK, Vanneste S, Beeckman T. 2016. Cyclic programmed cell death stimulates hormone signaling and root development in Arabidopsis. *Science* **351**, 384-387.

Xue X, Fry SC. 2012. Evolution of mixed-linkage (1 → 3, 1 → 4)-β-d-glucan (MLG) and xyloglucan in Equisetum (horsetails) and other monilophytes. *Annals of Botany* **109**, 873-886.

Zverlov VV, Schantz N, Schmitt-Kopplin P, Schwarz WH. 2005. Two new major subunits in the cellulosome of Clostridium thermocellum: xyloglucanase Xgh74A and endoxylanase Xyn10D. *Microbiology* **151**, 3395-3401.